

Electronic Thesis and Dissertation Repository

8-17-2023 1:00 PM

Role of Circular RNA ASPH in Macrophage Polarization and Response in Sepsis

Tan Ze Wang, *Western University*

Supervisor: Zheng, Xiufen, *The University of Western Ontario*

A thesis submitted in partial fulfillment of the requirements for the Master of Science degree in Pathology and Laboratory Medicine

© Tan Ze Wang 2023

Follow this and additional works at: <https://ir.lib.uwo.ca/etd>



Part of the [Immune System Diseases Commons](#), and the [Medical Immunology Commons](#)

Recommended Citation

Wang, Tan Ze, "Role of Circular RNA ASPH in Macrophage Polarization and Response in Sepsis" (2023). *Electronic Thesis and Dissertation Repository*. 9528.
<https://ir.lib.uwo.ca/etd/9528>

This Dissertation/Thesis is brought to you for free and open access by Scholarship@Western. It has been accepted for inclusion in Electronic Thesis and Dissertation Repository by an authorized administrator of Scholarship@Western. For more information, please contact wlsadmin@uwo.ca.

Abstract

Circular RNAs (circRNAs), a novel non-coding RNA species generated by back-splicing, have been shown to participate in gene regulation of leukocytes. Our previous RNA sequencing results show that circular RNA ASPH (circASPH) is highly expressed in peripheral blood mononuclear cells of sepsis patients at the start of intensive care. Macrophages release cytokines to recruit other immune cells at sepsis onset, and dysregulation of macrophage polarization affects sepsis progression. This work investigates the role of circASPH in the regulation of macrophage polarization. Using an *in vitro* THP-1 cell model, it was found that circASPH levels peaked after 24 h of IFN- γ + LPS stimulation and after 12 h of IL-4 stimulation. Knockdown of circASPH prior to polarization resulted in downregulation of M1 gene expression and cytokine secretion. These results suggest a proinflammatory role of circASPH in macrophage polarization and imply its participation in sepsis pathogenesis.

Keywords

Sepsis, peripheral blood mononuclear cells, circular RNA, circASPH, macrophage polarization

Summary for Lay Audience

Sepsis is a life-threatening medical condition where the immune system overreacts to an infection and damages other organs. The majority of people who die from an infection develop sepsis, yet there is currently no reliable treatment to reduce the immune response in sepsis. Macrophages are a type of immune cell that can perform a variety of functions, from killing bacteria and viruses to cleaning up cellular debris and helping with tissue repair. They are first responders during an infection and release signals to other immune cells.

Macrophage polarization is the term describing a macrophage's choice to produce signals that increase or decrease the body's immune response, which is important in the development of sepsis. Many biological signals in and around the macrophage can affect its polarization.

Circular RNAs (circRNA) are a recently discovered type of molecule that can affect a cell's function. CircRNAs differ from other RNAs by forming a closed loop, which make them last longer in the body to carry out their effects. We have previously found a circRNA called circRNA ASPH (circASPH), that is present in high amounts in the immune cells of sepsis patients. The role of circASPH in macrophage polarization has not been studied before. My research shows that circASPH can affect macrophage polarization. I found that macrophages with more circASPH released more inflammatory signals to promote a stronger immune response. This work will help identify potential new targets in immune cells to control their responses, which will help us develop more robust and specific treatments to combat sepsis.

Acknowledgments

I would like to thank my supervisor Dr. Xiufen Zheng, for her invaluable mentorship, support, and guidance throughout the experimental design, data collection and analysis, and the writing of this thesis. I would like to thank my advisory committee members, Dr. Mansour Haeryfar and Dr. Tina Mele, for sharing their expertise and providing critique and suggestions to enrich my study. I would like to thank my lab members Adam Greasley, Shuailong Li, Amal Abu Omar, Samantha Collings, Serina Chahal, Danielle Taray-Matheson, Raj Thapa, and Tahereh Kashkoulnejad Kouhi for their companionship and support in the lab every day. Finally, I would like to thank the ICU research team at University Hospital, including Dr. Tina Mele, Tracey Bentall, and Courtney Hooper, for their help in coordinating the collection of the patient samples, as well as all the patients who participated in the sepsis study, without whom this work would not be possible.

Table of Contents

Abstract.....	ii
Summary for Lay Audience.....	iii
Acknowledgments.....	iv
Table of Contents.....	v
List of Tables.....	viii
List of Figures.....	ix
List of Supplemental Material.....	xi
List of Abbreviations.....	xii
Chapter 1.....	1
1 Introduction.....	1
1.1 Sepsis.....	1
1.1.1 Pathogenesis.....	1
1.1.2 Clinical diagnosis.....	3
1.1.3 Biomarkers.....	3
1.1.4 Current treatments.....	4
1.1.5 Immune cell dysfunction in sepsis.....	4
1.2 Macrophages.....	7
1.2.1 Macrophage polarization.....	9
1.2.2 Mechanism of macrophage polarization.....	11
1.2.3 Role of macrophages in sepsis.....	12
1.2.4 THP-1 cells as a model of macrophage function.....	13
1.3 Circular RNA: a brief overview.....	14
1.3.1 Circular RNAs in sepsis immunopathology.....	19

1.3.2	Circular RNAs in macrophages	20
1.4	Circular RNA ASPH.....	21
1.4.1	Circular RNA ASPH.....	21
1.4.2	ASPH gene transcripts and function	23
1.5	Hypothesis Statement.....	24
Chapter 2	25
2	Materials and Methods.....	25
2.1	Septic PBMC sample collection	25
2.2	Total RNA extraction.....	25
2.3	cDNA synthesis	26
2.4	Quantitative Polymerase Chain Reaction (qPCR)	26
2.5	Cell culture.....	28
2.5.1	THP-1 model of macrophage polarization.....	28
2.6	RNA-Fluorescence in situ Hybridization.....	28
2.7	Transfection	30
2.8	Cell death assay.....	30
2.9	Western blotting.....	31
2.10	Multiplex cytokine assay	33
2.11	Statistical analysis.....	33
Chapter 3	35
3	Results.....	35
3.1	CircASPH is overexpressed in PBMCs at ICU admission	35
3.2	CircASPH expression level in septic PBMCs correlates with plasma cytokine levels of IL-12p70 and IL-5	37
3.3	PMA induces IL-1 β expression during differentiation of THP-1 macrophages...	41

3.4	Alteration in expression of circASPH isoforms between THP-1 monocytes and macrophages	43
3.5	Validation of macrophage polarization model.....	45
3.6	Alteration of circASPH and ASPH expression by cytokine stimulation.....	47
3.7	CircASPH is primarily localized in the cytoplasm.....	51
3.8	CircASPH siRNA knocks down circASPH expression.....	54
3.9	CircASPH siRNA downregulates M1 genes and upregulates M2 genes	55
3.10	CircASPH knockdown attenuates cytokine secretion during M1 polarization	58
3.11	CircASPH knockdown reduces STAT1 protein expression	60
3.12	CircASPH knockdown does not increase cell death.....	62
Chapter 4	64
4	Discussion and Conclusion	64
4.1	CircASPH upregulated in septic PBMCs at ICU-AD and associated with IL-12 and IL-5 secretion	64
4.2	CircASPH expression in THP-1 model of macrophage polarization	66
4.3	CircASPH knockdown reduces M1 cytokine production and STAT1 expression	68
4.4	Pretreatment with circASPH siRNA and M2 polarization	70
4.5	ASPH	70
4.6	CircASPH and cell death	71
4.7	Limitations	72
4.8	Concluding Remarks and Future Directions.....	73
Chapter 5	74
5	References	74
	Supplementary Material.....	85
	Curriculum Vitae	89

List of Tables

Table 1.1 Immune cell function and examples of dysregulation in sepsis	5
Table 1.2 Subtypes of alternatively-activated macrophages.....	11
Table 2.1 Primer sequences used for qPCR.....	27
Table 2.2 Recipe for pre-hybridization buffer for RNA-FISH.....	29
Table 2.3 Recipe for 5x saline sodium citrate buffer.....	30
Table 2.4 List of primary antibodies used for western blotting.....	33
Table 3.1 Correlation results between circASPH and plasma cytokine levels before and after intensive care	39

List of Figures

Figure 1.1 The biphasic model of sepsis pathogenesis.	2
Figure 1.2 Schematic for biogenesis of monocyte-derived and tissue resident macrophages..	8
Figure 1.3 CircRNA structure and biogenesis	16
Figure 1.4 Schematic of circular RNA putative functions.....	18
Figure 1.5 Schematic for the two isoforms of circASPH.	22
Figure 3.1 CircASPH overexpressed in septic PBMCs before intensive care.....	36
Figure 3.2 Overexpression of cytokines in sepsis patients at the start of intensive care.	38
Figure 3.3 CircASPH correlates with IL-12 at ICU-AD and IL-5 at ICU-DC.....	40
Figure 3.4 PMA induces IL-1 β expression during THP-1 differentiation.....	42
Figure 3.5 PMA removal alters circASPH expression.	44
Figure 3.6 Cytokine stimulation induces THP-1 macrophage polarization gene markers.	46
Figure 3.7 CircASPH and ASPH levels fluctuate during THP-1 macrophage M1 polarization.	48
Figure 3.8 CircASPH levels fluctuate while ASPH is elevated during THP-1 macrophage M2 polarization.	50

Figure 3.9 CircASPH is primarily expressed in the cytosol of PMA-treated THP-1 cells by RNA-FISH with Cyanine 5-labelled probes.	52
Figure 3.10 CircASPH upregulation in polarized THP-1 macrophages determined by RNA-FISH.	53
Figure 3.11 Transfection with anti-circASPH siRNA attenuates circASPH expression.	54
Figure 3.12 CircASPH knockdown attenuates the expression of IFN- γ + LPS-stimulated M1 gene markers.	56
Figure 3.13 Pre-transfection with circASPH siRNA upregulates IL-4-stimulated M2 gene marker expressions.	57
Figure 3.14 CircASPH knockdown reduces cytokine production during M1 polarization. ...	59
Figure 3.15 CircASPH knockdown reduces STAT1 protein during M1 polarization.	61
Figure 3.16 Cell death curve of PMA-treated THP-1 cells after circASPH knockdown and IFN- γ + LPS treatment.	63

List of Supplemental Material

Table S1 Patient demographic and clinical information.....	85
Figure S1 Validation of PCR products for 18S, circASPH and ASPH.	86
Figure S2 Validation of PCR products for M1 and M2 gene markers..	87
Figure S3 CircASPH siRNA binding to circASPH and linear ASPH.	88

List of Abbreviations

ALOX15	arachidonate 15-lipoxygenase
ARDS	acute respiratory distress syndrome
ASPH	aspartate β -hydroxylase
ATCC	American Type Culture Collection
BSA	bovine serum albumin
BSJ	backsplice junction
CCL17	CC motif chemokine ligand 17
CD	cluster of differentiation
cDNA	complementary DNA
circRNA	circular RNA
circASPH-1	circular RNA ASPH isoform 1
circASPH-2	circular RNA ASPH isoform 2
CXCL	chemokine (C-X-C motif) ligand
Cy5	cyanine-5
DAPI	4',6-diamidino-2-phenylindole
EDTA	ethylenediaminetetraacetic acid
GM-CSF	granulocyte-macrophage colony-stimulating factor
ICU	intensive care unit
ICU-AD	admission into intensive care unit

ICU-DC	discharge from intensive care unit
IFN	interferon
I κ B	inhibitor of NF- κ B
IL	interleukin
JAK	Janus kinase
LPS	lipopolysaccharide
M1 macrophage	classically-activated macrophage
M2 macrophage	alternatively-activated macrophage
MCP-1	monocyte chemoattractant protein-1
miRNA	microRNA
NC	negative control
NF- κ B	nuclear factor-kappa B
NK cells	natural killer cells
PBMC	peripheral blood mononuclear cell
PBS	phosphate-buffered saline
PBS-T	phosphate-buffered saline containing 0.1% Tween® 20
PI	propidium iodide
PMA	phorbol 12-myristate 13-acetate
PMSF	phenylmethanesulfonyl fluoride
qPCR	quantitative polymerase chain reaction

qRT-PCR	quantitative reverse transcription polymerase chain reaction
RBP	RNA binding proteins
RNA-FISH	RNA-fluorescent <i>in situ</i> hybridization
RNAseq	RNA-sequencing
ROS	reactive oxygen species
RPMI-1640	Roswell Park Memorial Institute-1640
RT	room temperature
si-circASPH	anti-circASPH siRNA
STAT	signal transducer and activator of transcription
TGF- β	transforming growth factor-beta
Th	T helper (cell)
TLR	Toll-like receptor
TNF- α	tumor necrosis factor alpha

Chapter 1

1 Introduction

1.1 Sepsis

Sepsis is defined as “a life-threatening organ dysfunction caused by a host’s dysfunctional response to infection”¹. It is the most common cause of death from infection¹ and a major global health burden, with an estimated 48.9 million incident cases and 11 million sepsis-related deaths worldwide in 2017². Sepsis affects up to 1–2% of all hospitalized patients, and it is a major cause of death in the intensive care unit (ICU)³. Patients of any age group may develop sepsis, but children, neonates, and older patients are especially vulnerable². Sepsis is much more prevalent in developing countries, with around 85% of cases occurring in countries with low social development index². However, sepsis remains a major burden in the aging and immunodeficient populations in high-income countries.

1.1.1 Pathogenesis

Sepsis has long been considered a biphasic disease, characterized by an initial hyperinflammatory phase for several days followed by a long-term immunosuppressive phase (Figure 1.1)⁴. The hyperinflammatory phase can be triggered by a bacterial, viral, or fungal infection that enters the blood, or even by tissue trauma⁵. It is characterized by hypermetabolism, fever, and the excessive production of pro-inflammatory cytokines such as tumor necrosis factor-alpha (TNF- α) and interleukin-1 (IL-1), leading to a systemic inflammatory response^{4,6}. This “cytokine storm” drives immune activation throughout the body, and incites widespread endothelial cell activation, causing increased

vascular permeability and reduced blood flow to vital organs ⁷. Both hyperinflammation and endothelial dysfunction ultimately lead to multiple organ dysfunction syndrome, the severity of which is the primary factor in determining sepsis outcome and prognosis ¹. Among survivors of sepsis, immune dysregulation continues in the form of life-long immune suppression, characterized by apoptotic depletion of effector immune cells and relative increase of immunosuppressive cells and cytokines ⁶. This leads to increased susceptibility to secondary infections, a major cause of increased morbidity in sepsis survivors ⁴.

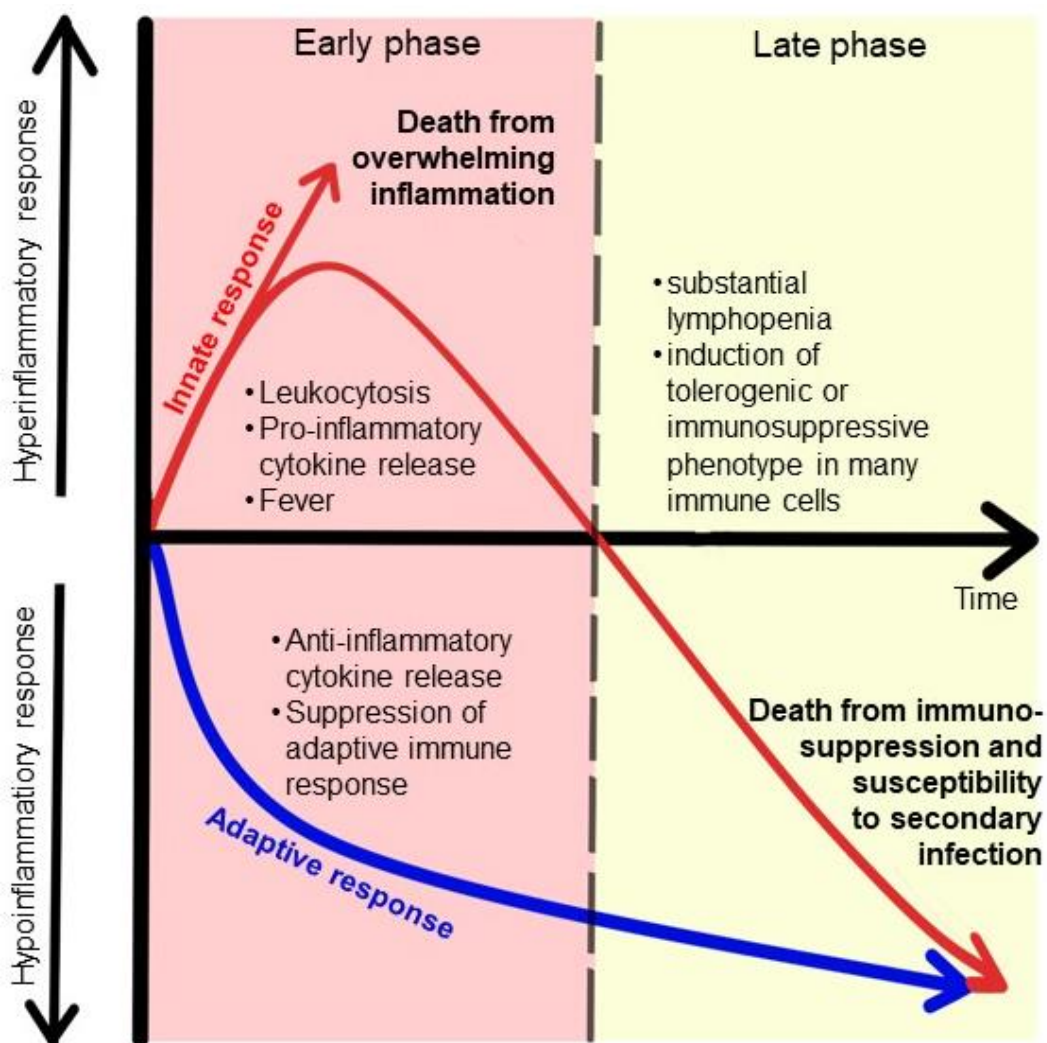


Figure 1.1 The biphasic model of sepsis pathogenesis.

In the early 2010s, repeated failures of anti-inflammatory therapy for sepsis led to the discovery that many patients exhibit high levels of anti-inflammatory cytokines or lower levels of all cytokines in the early phase of sepsis ⁶. Since then, the importance of immunosuppression in the early phase of sepsis became of increasing research interest.

1.1.2 Clinical diagnosis

The most recent definition of sepsis emphasizes organ dysfunction as the primary contributor of sepsis morbidity and mortality ¹. As such, sepsis is diagnosed with 2 points on the Sequential Organ Failure Assessment score for a patient in the ICU, or 2 out of 3 positive diagnoses on the quick Sequential Organ Failure Assessment for a patient outside the ICU ¹. Septic shock is a more severe subset of sepsis characterized by substantial circulatory, cellular, and metabolic abnormality, with a hospital mortality of greater than 40% ¹. Septic shock should be diagnosed in sepsis patients with hypotension requiring vasopressors and hyperlactatemia ¹.

1.1.3 Biomarkers

Established biomarkers for sepsis diagnosis and monitoring prognosis include procalcitonin, C-reactive protein, TNF- α , IL-6, monocyte chemoattractant protein-1 (MCP-1), and complement proteins ³. Research has also suggested the use of monocytic surface proteins such as programmed death receptor-1, soluble triggering receptor expressed on myeloid cells-1, cluster of differentiation 64 (CD64), and presepsin (cleaved subtype of soluble CD14) ³. There is also evidence suggesting the use of microRNA (miRNA) and plasma cell-free DNA as efficacious biomarkers to determine sepsis diagnosis and prognosis ³.

1.1.4 Current treatments

Currently, there is no FDA-approved pharmacological intervention specific for sepsis³, despite more than 100 clinical trials attempting anti-endotoxin, anti-cytokine, or anti-apoptotic therapies⁵. The best practice recommendations for sepsis treatment include early detection of inflammatory biomarkers and timely administration of appropriate antimicrobial targeting the inciting infection if possible, along with supportive therapies such as mechanical ventilation, blood glucose level management, and vasopressor therapy⁸. Empiric broad-spectrum antimicrobial therapy is recommended to start within an hour of diagnosis if early pathogen identification is not possible, but the patient should be reassessed daily to avoid unnecessary use of multidrug therapy⁸. Use of corticosteroids, immunoglobulins, and anticoagulants are not recommended, as they lack support from clinical trials⁸. Sedation should also be minimized to avoid prolonging of mechanical ventilation and to allow earlier mobilization⁸.

1.1.5 Immune cell dysfunction in sepsis

As a disease of immune dysfunction, there has been extensive research regarding the role of each immune cell type during sepsis. Upon infection, innate immune cells, such as neutrophils and macrophages respond immediately to fight the infection, while dendritic cells process microbial antigens to activate the adaptive immune system. Adaptive immune cells, including T and B cells, then mount a delayed but powerful antigen-specific immune response while also generating memory cells for future responses to the same antigen. A non-exhaustive list of immune cell activity and dysfunction in sepsis can be found in Table 1⁷. However, such research has also revealed significant heterogeneity in the presentation of sepsis patients. Seigel and colleagues found that among patients

with proven bacteremia, 52% showed a normal white blood cell count, indicating the limited effectiveness of the mandatory white blood cell count in predicting sepsis ⁹. Hoser and colleagues performed absolute counts of white blood cell types in sepsis patients of intraabdominal and pneumonia origin, and while they found significantly elevated overall leukocyte and granulocyte count and decreased T, B, and natural killer (NK) cells for both types of sepsis patients, they observed a two-fold increase in monocyte count in intraabdominal sepsis patients compared with controls, while there was a 30% decrease in monocyte count in pneumonia-derived sepsis patients ¹⁰. Such heterogeneity in sepsis pathophysiology remains a major obstacle in the discovery of reliable biomarkers for early sepsis diagnosis.

Table 1.1 Immune cell function and examples of dysregulation in sepsis

Cell type	Function during infection	Dysregulation in Late stage sepsis
Neutrophil	<ul style="list-style-type: none"> • Responds to cytokines from APCs • Proliferation • Production of reactive oxygen species 	<ul style="list-style-type: none"> • Proliferation of immature neutrophils • Apoptosis of mature neutrophils • Increased extravasation, ROS production, and NET formation • Reduced TNF-α, IFN-γ, IL-4 production; increased IL-10
Monocyte/ Macrophage	<ul style="list-style-type: none"> • Initiates immune response • Phagocytosis of pathogen • Proliferation • Activation by IL-1β 	<ul style="list-style-type: none"> • Endotoxin tolerance • Increased apoptosis • Reduced antigen presentation • Reduced TNF-α, IL-1β, IL-6 production; unchanged or increased IL-10
Dendritic cells	<ul style="list-style-type: none"> • Initiates immune response • Phagocytosis of pathogen • Presents antigens to lymphocytes 	<ul style="list-style-type: none"> • Marked reduction in number through apoptosis • Reduced antigen presentation • Reduced TNF-α, IL-12 production; increased IL-10 and TGF-β

Table 1.1 continued

Cell type	Function during infection	Dysregulation in Late stage sepsis
NK cells	<ul style="list-style-type: none"> • Direct killing of abnormal cells • IFN-γ production to stimulate macrophages 	<ul style="list-style-type: none"> • Reduction in number through apoptosis • Reduced cytotoxic function and endotoxin response • Reduced TNF-α, IFN-γ , IL-18 production
CD4 ⁺ T cells	<ul style="list-style-type: none"> • Activates other immune cells • Th1 cells produce IFN-γ • Th2 cells produce IL-4, IL-5, and IL-10 • Th1 and Th2 cells produce IL-3 to stimulate myeloid cell production 	<ul style="list-style-type: none"> • Marked reduction in number through apoptosis • Imbalance of Th1/Th2 cytokines causes vulnerability to secondary infections • Reduced TCR diversity
CD8 ⁺ T cells	<ul style="list-style-type: none"> • Direct killing of infected or abnormal cells • Releases TNF-α and IFN-γ • Generates memory cells 	<ul style="list-style-type: none"> • Marked reduction in number through apoptosis • Reduced cytokine production and cytotoxic activity • Reduced TCR diversity
Regulatory T cells	<ul style="list-style-type: none"> • Controls immune response and maintains tissue homeostasis 	<ul style="list-style-type: none"> • Relative increase in number through apoptosis resistance • Increased anti-inflammatory markers and cytokine production
B cells	<ul style="list-style-type: none"> • Antibody production • Enhance innate response through IFN receptor 	<ul style="list-style-type: none"> • Marked reduction in number through apoptosis • Exhaustion • Reduced antibody production

As the focus of understanding sepsis pathogenesis shifted from uncontrolled inflammation to the dysregulation between pro- and anti-inflammatory responses, greater emphasis was placed on the altered gene expression in blood leukocytes at sepsis onset. A pioneering study comparing the genomic response of blood leukocytes after severe trauma, burn injury, and endotoxemia found significant alteration in up to 80% of the leukocyte transcriptome manifesting within 12 h of injury ¹¹. These changes were similar

across all three types of injury, and generally involved an upregulation of innate immune response and downregulation of adaptive immune response ¹¹. Since then, many studies have performed transcriptome profiling of septic leukocytes at ICU admission (ICU-AD) to define molecular subgroups of sepsis patients and predict clinical outcome ^{12,13}. A recent study identified 4 genes that were significantly altered in the blood leukocytes of sepsis patients exhibiting early immunosuppression, and their expression were associated with hospital mortality ¹⁴. With the rise of single-cell sequencing in the last decade, studies in both mice ¹⁵ and human ¹⁶ have characterized the transcriptomic landscape of immune cells in sepsis, allowing quantification of changing cell subpopulations and identification of biological pathways affected in sepsis. These results suggest that further research into the leukocyte gene regulation underlying sepsis may create novel avenues of drug discovery for this life-threatening syndrome.

1.2 Macrophages

Macrophages are ubiquitous sentinel immune cells that play critical roles in both innate and adaptive immunity. Tissue macrophages are long thought to be terminally differentiated cells that were primarily derived from circulating monocytes, which are themselves derived from myeloid progenitor cells in the bone marrow (Figure 1.2) ¹⁷. However, recent studies have highlighted the importance of circulation-independent ontogeny of tissue macrophages, which derive from embryonic precursors and self-renew well into adulthood in the absence of infections (Figure 1.2) ¹⁸. In old age, resident macrophages in several tissues, such as the kidneys, intestines, and the heart, are replaced by monocyte-derived macrophages ¹⁷. Tissue macrophages further specialize into specific macrophage subsets to fulfill the homeostatic needs of their niche. Examples of

macrophage subsets include the microglia in the central nervous system, the Kupffer cells in the liver, and osteoclasts in the bone ¹⁷.

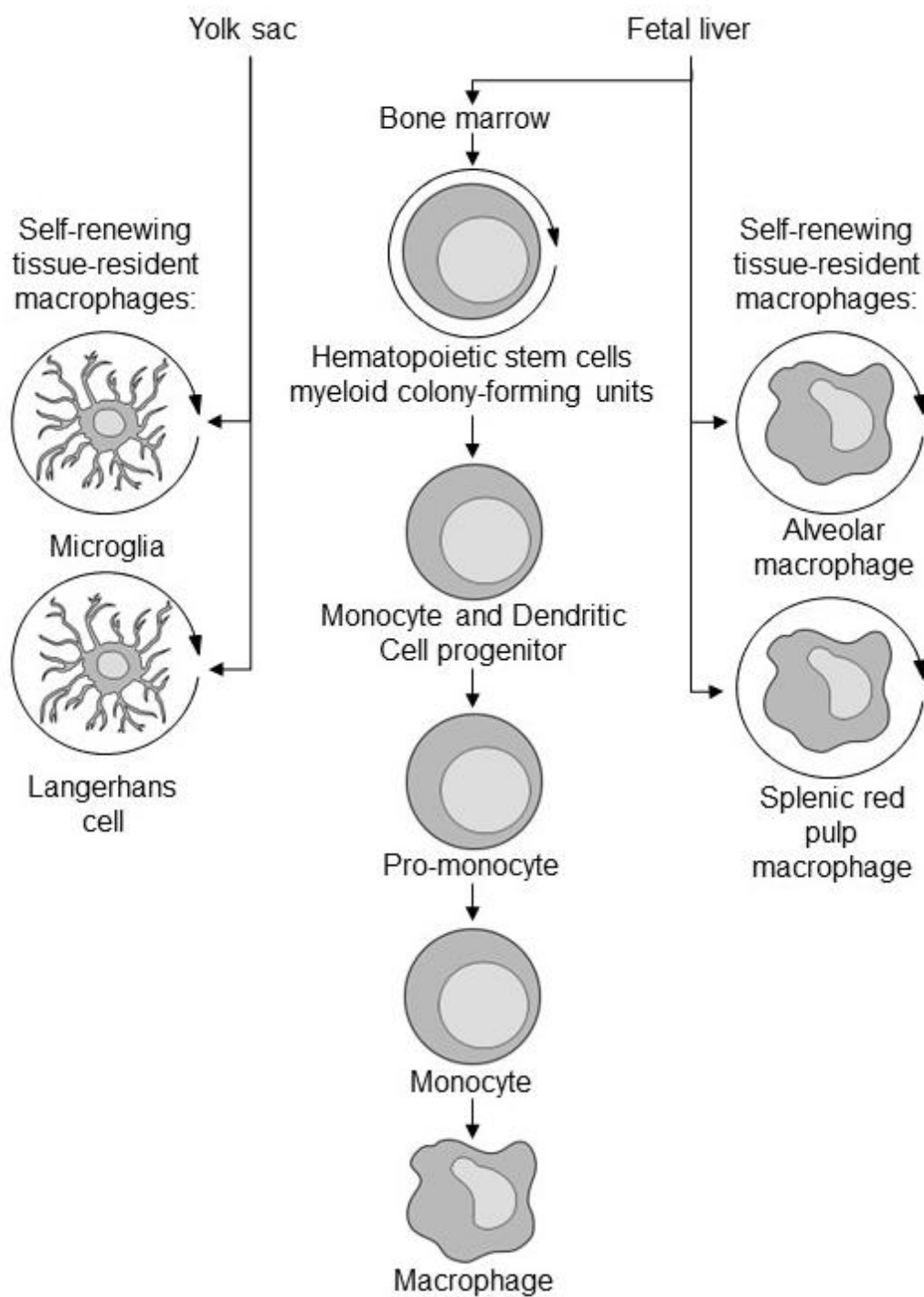


Figure 1.2 Schematic for biogenesis of monocyte-derived and tissue resident macrophages.

The primary function of macrophages is phagocytosis, where they engulf and digest substances that are non-self. In sepsis, macrophages are first-line responders to infection, and they recognize pathogens through pattern recognition receptors that bind to pathogen-associated molecular patterns on microbes, such as lipopolysaccharide (LPS). The macrophage engulfs its target through receptor-mediated endocytosis into a phagosome, which then fuses with a lysosome, containing enzymes and reactive oxygen species (ROS) that break down the engulfed material ¹⁹. Furthermore, macrophages are activated by interactions with pathogens or by environmental cytokines, and they produce a plethora of cytokines and chemokines in response, which control the immune response by mediating the recruitment and activation of other immune cells ¹⁹.

Outside the context of an infection, macrophages also participate in tissue remodeling and wound repair through phagocytosis of cellular debris and the production of growth factors and extracellular matrix components ¹⁹.

1.2.1 Macrophage polarization

Activated macrophages can adopt different functional phenotypes based on environmental stimuli, a phenomenon termed macrophage polarization. Understanding of macrophage polarization began with the discovery that T helper 2 (Th2) cytokines IL-4 and IL-13 induces mannose receptor expression in macrophages and reduces pro-inflammatory cytokine production ²⁰. Two distinct types of polarized macrophages were first described in 2000 by Mills and colleagues in their investigation of macrophage arginine metabolism: classically-activated (M1) and alternatively-activated (M2) macrophages ²¹.

M1 macrophages are induced by pro-inflammatory signals such as toll-like receptor (TLR) ligands and interferon-gamma (IFN- γ). They undergo metabolic reprogramming, downregulating oxidative phosphorylation in favour of the less efficient but faster glycolysis through hypoxia-inducible factor-1 α and mammalian target of rapamycin²². M1 macrophages have increased phagocytic capabilities, and produce proinflammatory cytokines such as TNF- α , IL-1 β , IL-6, chemokine (C-X-C motif) ligand 9 (CXCL9), CXCL10, IL-12, and IL-23^{19,23}. They are also professional antigen presenting cells, able to process and display extracellular antigens on major histocompatibility complex class II molecules. This allows them to activate T and B lymphocytes to mount a stronger adaptive immune response. M1 macrophages are key effector cells in the initiation and amplification of an immune response against pathogens.

M2 macrophages are induced by anti-inflammatory signals such as IL-4 or IL-13. They produce anti-inflammatory cytokines such as IL-10, transforming growth factor-beta (TGF- β), and CC motif chemokine ligand 17 (CCL17), they participate in tissue remodeling and immune regulation¹⁷. M2-polarized macrophages are also metabolically distinct from M1 macrophages. For example, the enzyme arachidonate 15-lipoxygenase (ALOX15) is induced by IL-4 stimulation²³. In the resolution phase of an inflammatory response, M2 macrophages play a crucial role in suppressing the immune response and initiating tissue repair, angiogenesis, and restoring homeostasis¹⁹.

Recent studies have characterized subtypes within the M2 macrophage phenotypes, such as M2a, M2b, M2c, and M2d (Table 2)¹⁷. It is now accepted that the various phenotypes of activated macrophages should be viewed on a spectrum, and that macrophages *in vivo* are a heterogenous population with diverse phenotypes and functional states depending

on their microenvironmental signals ¹⁷. Macrophages in diseased states may also exhibit phenotypes that deviate from the aforementioned categories. Dysregulation of macrophage polarization is thought to contribute to various immune-mediated diseases.

Table 1.2 Subtypes of alternatively-activated macrophages

Subtype	Stimulus	Markers	Cytokines produced	Role
M2a	IL-4, IL-13	CD163, CD206, CD209	IL-10, TGF- β , CCL17, CCL24, CSF-1	Anti-inflammation, tissue repair
M2b	LPS, immune complexes	CD206, MHCII, CD86	Pro- and anti-inflammatory cytokines	Anti-inflammation, pro-tumor and infection
M2c	IL-10, TGF- β	CD206, CD163, MerTK	IL-10, CCL18, CXCL13, TGF- β	tissue homeostasis by phagocytosis of apoptotic cells
M2d	TLR agonist, IL-6	CD206	IL-10, CCL18, CCL22	Pro-tumour, angiogenesis

1.2.2 Mechanism of macrophage polarization

Macrophage polarization is regulated by a complex network of signaling pathways that work together to regulate the expression of effector genes and drive changes in macrophage phenotype.

1.2.2.1 TLR4/NF- κ B pathway

Macrophages are activated by pathogen-associated molecular patterns, such as LPS, through the TLR4/nuclear factor-kappa B (NF- κ B) pathway, which is a strong driver for M1 polarization. TLR4 is a surface receptor that binds LPS, forming a complex with the protein myeloid differentiation factor 2 with the help of CD14 ²⁴. This complex triggers a signaling cascade through the myeloid differentiation primary response 88-dependent pathways, and ultimately leads to the phosphorylation and activation of inhibitor of NF-

κ B (I κ B) kinases. I κ B normally binds NF- κ B, keeping it inactivated and sequestered in the cytoplasm. Phosphorylation of I κ B leads to its degradation, allowing NF- κ B to translocate into the nucleus and induces the expression of pro-inflammatory genes ²⁴.

NF- κ B is a hetero- or homo-dimer composed of many possible subunits: RelA/p65, c-Rel, RelB, p50, and p52. Of these subunits, RelA/p65 is the most well-characterized, containing a transactivation domain that confers transcriptional abilities to NF- κ B. I κ B kinases are also responsible for the phosphorylation of the S536 residue on RelA/p65, which enhances its transactivation functions ²⁵.

1.2.2.2 JAK/STAT pathway

Macrophages are activated by cytokines primarily through the Janus kinase (JAK)/signal transducer and activator of transcription (STAT) pathway. JAK is normally bound to cytokine receptors, and are phosphorylated when the receptor binds to its ligand. JAK then induces STAT phosphorylation, which causes STAT dimerization and translocation to the nucleus to induce effector gene expression ²⁶. There are 4 JAKs and 7 STATs currently known, and different cytokines activate different STATs for their effector functions. For example, the IFN- γ receptor activates STAT1 to induce pro-inflammatory genes, while the IL-4 and IL-13 receptors activate STAT6 to induce anti-inflammatory genes ²⁷.

1.2.3 Role of macrophages in sepsis

Macrophages play a crucial role in both the hyperinflammatory and immunosuppressive stages of sepsis. In the early stage of sepsis, the primary role of macrophages is phagocytosis of pathogens to clear the infection. Macrophages respond to IFN- γ from T

cells through the STAT1 pathway and upregulate the release of proinflammatory cytokines, contributing to the progression of cytokine storm²⁸. In the later stage of sepsis, macrophages become exhausted through endotoxin tolerance and repeated exposure to apoptotic cells⁵. Endotoxin tolerance is likely driven by a combination of metabolic shifts from glycolysis to oxidative phosphorylation²², and epigenetic changes in myeloid progenitors and monocytes²⁹. Endotoxin tolerant macrophages exhibit similar phenotypes to M2 polarization, including increased production of immunosuppressive cytokines and reduced antigen presentation, and they are major contributors to sepsis mortality^{4,30}. Restoring M1 phenotype and functions through either IFN- γ ^{31,32} or granulocyte-macrophage colony-stimulating factor (GM-CSF)³³ therapy have been shown to improve the long-term clinical outcomes of sepsis patients.

1.2.4 THP-1 cells as a model of macrophage function

The THP-1 cell line is an acute monocytic leukemia cell line extracted from a 1-year-old human male, expressing Fc and C3b receptors but no immunoglobulins³⁴. THP-1 cells can be differentiated by phorbol 12-myristate-13 acetate (PMA), a protein kinase C activator, into cells that mimic monocyte-derived macrophages³⁵. PMA-differentiated THP-1 cells show much greater sensitivity to LPS compared with undifferentiated THP-1 cells, due to greater expression of TLR4 and myeloid differentiation primary response 88, as well as higher phosphorylation levels in mitogen-activated protein kinases and NF- κ B pathway proteins³⁶. A recent study comparing THP-1 cells with U937 cells, another popular monocytic cell line, found that THP-1 cells were more responsive to M1 stimuli, showing greater capacity for M1 functions such as phagocytosis and ROS production, while U937 cells were more responsive to M2 stimuli³⁷.

PMA is commonly used at a concentration of 100 to 200 nM to differentiate THP-1 cells, and the resulting macrophage-like cells can be polarized towards an M1 phenotype by IFN- γ + LPS stimulation and towards an M2 phenotype by IL-4 stimulation³⁸. However, Maeß and colleagues reported that these PMA concentrations promote M1 polarization, which reduces the effectiveness of M2 stimuli. They showed that lowering the concentration of PMA improves M2 polarization of differentiated THP-1 cells, without reducing the response to M1 stimuli³⁹. Baxter and colleagues proposed the inclusion of a resting phase where the cells are kept in PMA-free media prior to cytokine stimulation to further improve M2 differentiation³⁸.

1.3 Circular RNA: a brief overview

Circular RNAs (circRNAs) are a novel class of non-coding RNAs characterized by a covalently closed circular structure without a 5' cap or poly-A tail (Fig. 1.3)⁴⁰.

CircRNAs were first observed in eukaryotic cells by electron microscopy in 1979, but were thought to be functionless byproducts of alternative splicing and low in abundance^{41,42}. It is only in the past decade, with the rapid improvement of next-generation RNA-sequencing (RNAseq) and circRNA identification pipelines, circRNAs were found to be abundant and biologically significant, being produced by over 10% of expressed genes in certain cells⁴³.

CircRNAs are generated through backsplicing (Fig. 1.3), a type of alternative splicing that differs from conventional linear alternative splicing but relies on the same splicing machinery⁴⁴. During post-transcriptional processing, conventional splicing and backsplicing take place in competition. Long flanking introns, inverted repeat elements, and certain *trans*-acting RNA binding proteins (RBPs) promote backsplicing activity⁴⁴.

While conventional splicing links an upstream splice donor site to a downstream splice acceptor site, backsplicing joins the downstream splice donor to an upstream splice acceptor, leading to circularization and the formation of the backsplicing junction (BSJ) (Figure 1.3)⁴⁵. The specific role of the spliceosome in regulation conventional and backsplicing remains unknown, though a model of spliceosome formation proposed by Li and colleagues attempts to explain conventional and backsplicing through the same mechanism of spliceosome recognition⁴⁶. They propose that the spliceosome recognizes and forms around the 5' splice site and the downstream branch point sequence in the intron preceding the 3' splice site, and that backsplicing involves spliceosome formation around the downstream 5' splice site and the branch point sequence in an upstream intron⁴⁶.

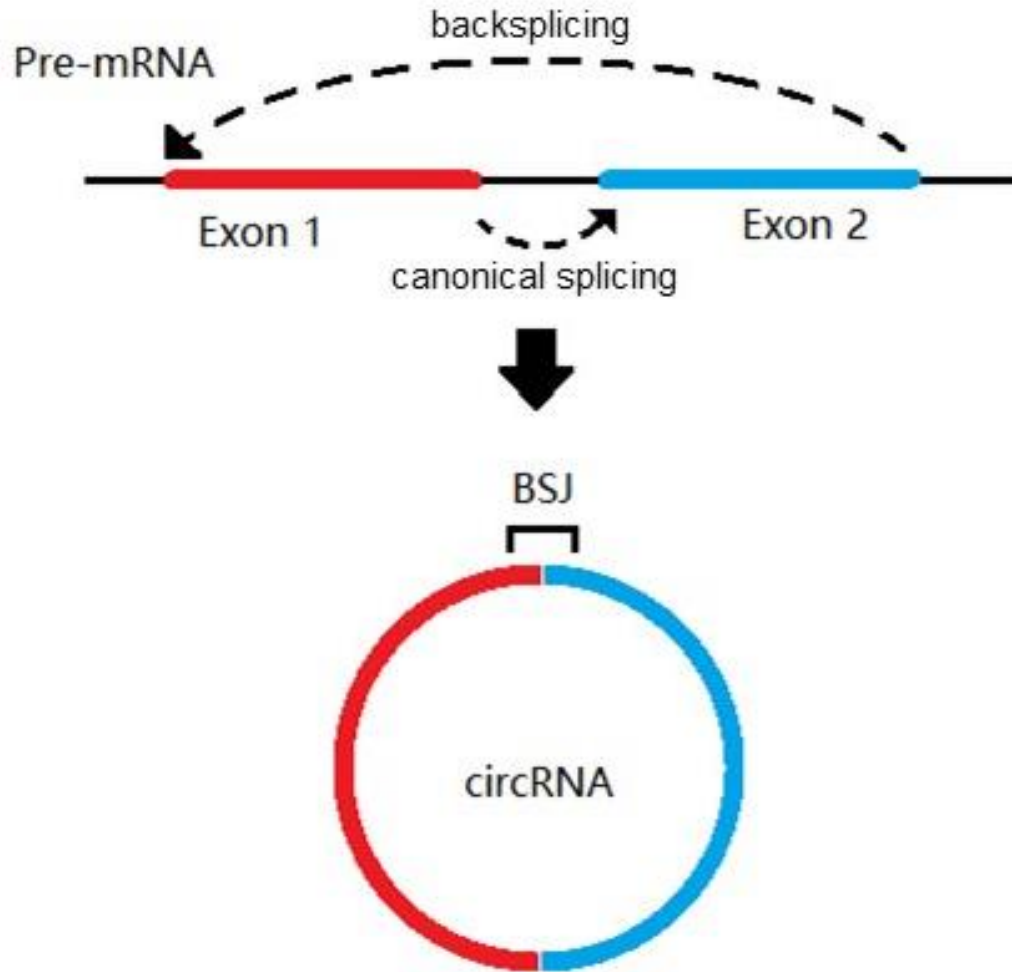


Figure 1.3 CircRNA structure and biogenesis

The majority of circRNAs comprise of only exon sequences, and are exported to the cytoplasm by RNA helicases DDX39A and DDX39B⁴⁴. However, a small proportion of circRNAs contains intron sequences, and those mostly remain in the nucleus^{44,47}.

CircRNAs exist in eukaryotic cells in much lower abundance overall compared to their linear counterparts, but they are highly stable due to their resistant to exonucleases^{43,44}.

CircRNAs are expressed in a cell type- or tissue-specific manner with no correlation to

the expression of their linear counterparts, with certain circRNAs being more highly expressed than their corresponding mRNAs in multiple cell lines⁴³. CircRNAs have also been found to be abundant and biologically relevant in plasma⁴⁸ and in exosomes⁴⁹, both of which are easily collected and analyzed in the clinic, conferring circRNAs great potential as biomarkers for diseases.

The recent explosion of research interest in circRNAs has identified numerous putative mechanisms whereby circRNAs regulate gene expression (Fig. 1.4). The most popular mechanism proposed is miRNA sponging, by which circRNAs compete with linear RNAs for miRNA binding and essentially sequester miRNAs due to their stability⁵⁰. The best known circRNA, ciRS-7, was named for its inclusion of over 60 miR-7 binding sites, and its conserved function across animal species^{51,52}. However, the majority of circRNAs have much fewer miRNA binding sites, and, coupled with their relative low abundance, are unlikely to function as miRNA sponges⁵³. CircRNAs can also interact with proteins in a number of ways, such as protein sponging, protein recruitment, or as structural support for protein complexes⁴⁴. A well-known example is circANRIL, expressed more than 10-fold higher than its linear counterpart in certain tissues, which binds pescadillo homologue 1 and impairs 60S-preribosomal assembly⁵⁴. As such, circANRIL induces p53 activation, halting proliferation and inducing apoptosis in vascular smooth muscle cells and macrophages, thus conferring protective effects in atherosclerosis⁵⁴. A few circRNAs are also shown to undergo cap-independent translation through an internal ribosome entry site, though peptides translated in this manner are often truncated, and likely serve purposes that differ from their full-length counterparts⁴⁴. Many studies have since investigated putative contributions of circRNAs to the pathogenesis of various

diseases, such as diabetes mellitus ⁵⁵, neurodegeneration ⁵⁶, and cancer ⁵⁷, highlighting the potential for circRNAs as targets for drug discovery or novel therapeutic strategies.

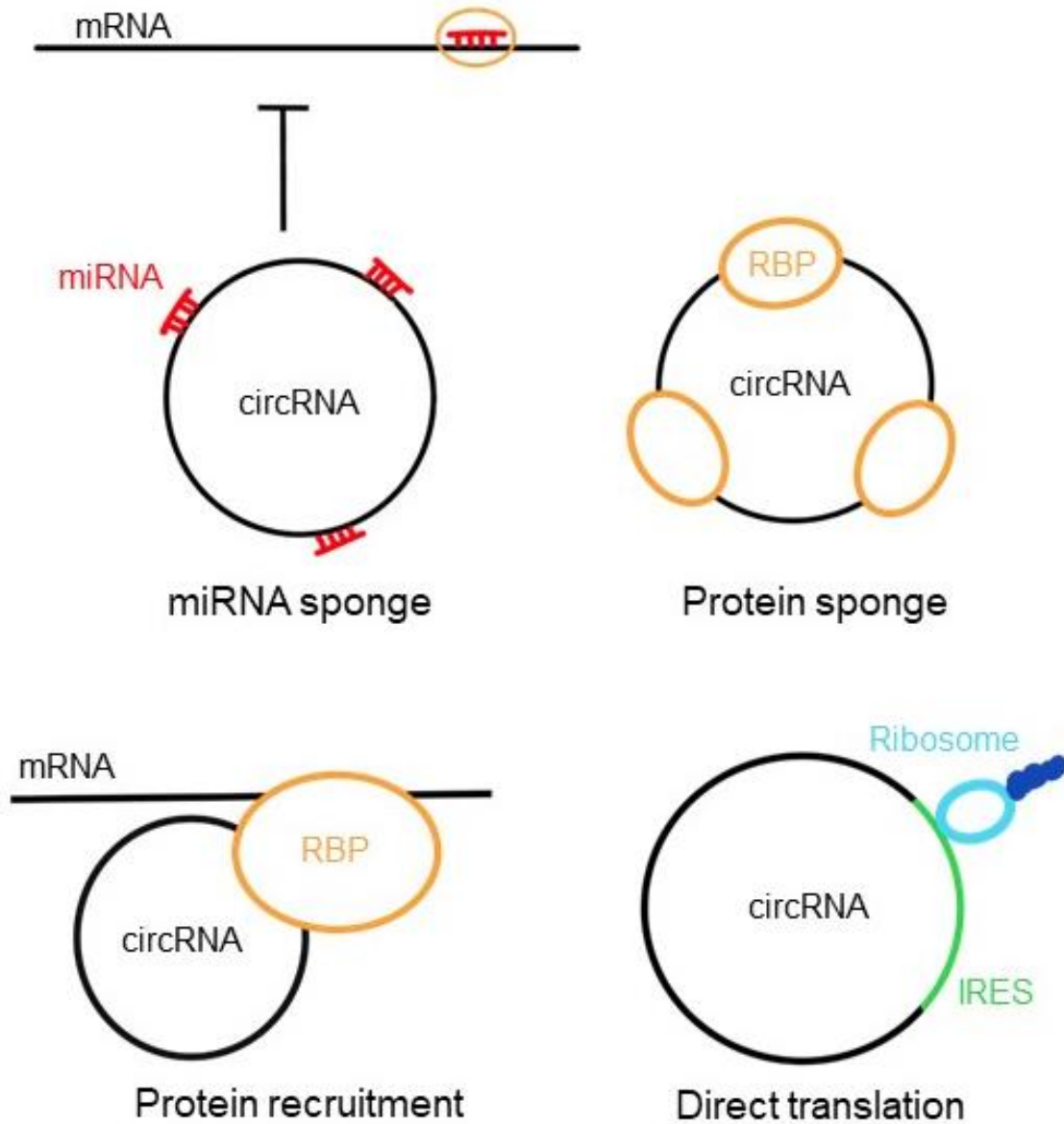


Figure 1.4 Schematic of circular RNA putative functions.

1.3.1 Circular RNAs in sepsis immunopathology

Emerging studies highlight the potential role of circRNAs in sepsis pathogenesis. Their abundance and stability makes them good biomarkers, and more than 20 circRNAs has been found to modulate immune-related mechanisms ⁵⁸. Nie and colleagues performed circRNA profiling in a rat model of sepsis and found 373 upregulated and 428 downregulated circRNAs in septic aortic tissue compared to normal controls ⁵⁹. Bao and colleagues profiled circRNA expression in alveolar macrophages isolated from a murine model of acute lung injury from sepsis; 11 upregulated circRNAs were identified, and are hypothesized to contribute to lung injury through sequestering miRNAs that promote M2 polarization ⁶⁰. Khan and colleagues found that PBMCs of sepsis patients secondary to community-acquired pneumonia produce more circRNA compared with healthy controls, and the circRNA landscape in each PBMC subtype is distinct ⁶¹. Guo and colleagues identified 14 co-differentially expressed circRNAs in the plasma and lung tissues of sepsis patients with acute respiratory distress syndrome (ARDS) compared with patients without ARDS, and these circRNAs are enriched in pathways involving adherens junction and extracellular matrix regulation ⁴⁰. Recently, Tian and colleagues have investigated the alteration of exosomal circRNAs in the serum of sepsis patients, and discovered two overexpressed circRNAs hsa_circRNA_104484 and hsa_circRNA_104670 that can potentially serve as novel biomarkers or therapeutic targets ⁶². Furthermore, Zhao and colleagues described a circRNA from the NEDD4 Binding Protein 1 gene that was shown to promote M1 polarization in murine pulmonary macrophages through miRNA sponging, thus exacerbating sepsis-induced ARDS ⁶³. However, most studies have focused on the alteration of circRNA expression between

septic PBMCs and healthy controls, and none have probed the difference in circRNA landscape between different stages of sepsis disease severity.

1.3.2 Circular RNAs in macrophages

The plasticity of macrophage polarization is controlled by an intricate network of signal pathways, and the importance of circRNAs in regulating macrophage function is increasingly recognized. Zhang and colleagues examined circRNA expression in bone marrow-derived macrophages, and reported 189 differentially expressed circRNAs between M1 and M2 polarized macrophages⁶⁴. Specific circRNA species have also been implicated in modulating macrophage function in bacterial infection^{65,66} and tuberculosis^{67,68}. Zhang and colleagues identified circPPM1F to promote M1 polarization through the NF- κ B pathway by downregulating its home gene, contributing to type 1 diabetes mellitus pathogenesis⁶⁹. Zhou and colleagues recently reported 71 upregulated and 69 downregulated circRNAs in M1-polarized THP-1 cells compared to M2, and identified a circRNA spliced from the Ring Finger Protein 19B gene to promote M1 polarization and inhibit M2 polarization, suggesting the potential role of circRNAs in regulating macrophage polarization⁷⁰.

Recognition of foreign circRNA by retinoic-acid-induced gene-I in innate immune cells is crucial to initiate an antiviral response. Endogenous circRNAs are recognized as self through introns and RBP-interactions, while exogenous circRNA sensing confers protection against viral infections⁷¹. Endogenous circRNA are also found to inhibit protein kinase R, another cytosolic nucleic acid receptor; upon viral infection, a global circRNA depletion by RNase L allows protein kinase R activation⁷². Overexpression of circRNA in PBMCs from systemic lupus erythematosus patients reduced protein kinase

R activation and type I IFN production, establishing a link between circRNAs and immunoregulation ⁷².

CircRNAs may directly participate in macrophage function. Xia and colleagues recently described a circRNA that was found to bind and inhibit cyclic GMP-AMP synthase, a cytosolic DNA sensor that can activate type I IFN production, to prevent an autoimmune response to self-DNA in bone marrow-derived macrophages ⁷³.

1.4 Circular RNA ASPH

1.4.1 Circular RNA ASPH

Our lab previously investigated the differential expression of circRNA in PBMCs from septic patients between the time of ICU-AD and discharge from ICU (ICU-DC) using RNAseq, and we identified a circRNA backspliced from the aspartate β -hydroxylase (ASPH) gene that was highly expressed and differentially expressed between ICU-AD and ICU-DC. This circRNA has two isoforms sharing the same BSJ, and comprises either exons 3 and 5 or exons 3, 4, and 5 of the ASPH pre-mRNA. The smaller isoform will be termed circASPH-1 herein, and the larger isoform circASPH-2 (Figure 1.4). CircASPH-2 is recorded in the database circBase as hsa_circ_0084615.

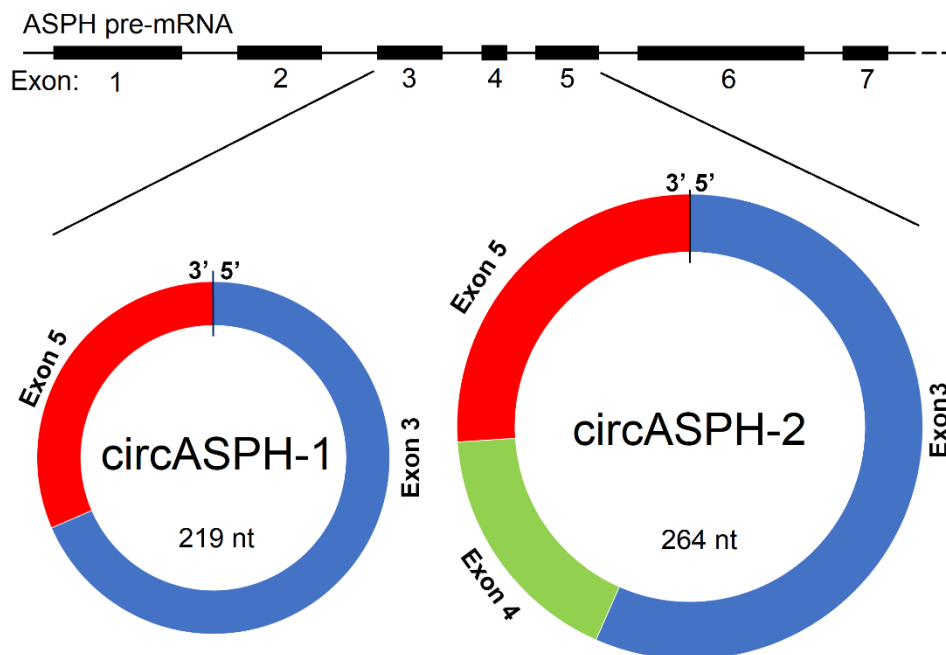


Figure 1.5 Schematic for the two isoforms of circASPH.

There are more than 30 circRNAs produced from the ASPH gene recorded in circBase, most of them having unique BSJs, and thus can be individually detected and may have entirely unrelated functions. However, they are currently poorly studied.

Hsa_circ_0009158, produced downstream from exons 9 to 18 in ASPH pre-mRNA (exons 4 to 13 of the ASPH mRNA) has been implicated in lung adenocarcinoma ⁷⁴, polycystic ovary syndrome ⁷⁵, and hepatic fibrosis ⁷⁶. In contrast, there are only two papers focusing on hsa_circ_0084615, or circASP-2, at the time of writing. Xu and colleagues described the oncogenic role of circASP-2 through sequestration of miR-581 and upregulating ATP-binding cassette transporter G1 in the context of cholangiocarcinoma ⁷⁷. Yi and colleagues described a similar mechanism in glioma where circASP-2 binds miR-599 and upregulates androgen receptor, which itself upregulates the oncogenic long non-coding RNA suppressor of cytokine signaling

2-antisense RNA 1⁷⁸. Nonetheless, there are currently no reports on the function of circASPH-1 or circASPH-2 in sepsis or macrophages.

1.4.2 ASPH gene transcripts and function

The ASPH gene undergoes extensive alternative splicing, generating at least 11 transcripts to ultimately produce three proteins with different functions: aspartyl- β -hydroxylase, junctin, and junctate^{79,80}. The enzyme aspartyl- β -hydroxylase catalyzes the hydroxylation of aspartic acid and asparagine residues in epidermal growth factor-like domains in many proteins, including Notch1 and TGF β 1^{79,81}. It contains an N-terminal cytoplasmic region, a universal transmembrane domain, a Ca²⁺ binding acidic luminal domain, and a C-terminal catalytic domain^{79,80}. Aspartyl- β -hydroxylase is expressed in many tissues⁸⁰, and it has an established oncogenic role in hepatocarcinoma and cholangiocarcinoma, where it is highly expressed and associated with decreased prognosis^{81,82}. Junctin is a structural protein found mainly in the sarcoplasmic reticulum of skeletal and cardiac muscles, and it contains a C-terminal basic luminal domain rather than the Ca²⁺ binding and catalytic domains, the shortest of the three proteins^{80,83}. Junctin interacts with calsequestrin, triadin, and ryanodine receptor to regulate Ca²⁺ release and myocyte contractility⁸³. Junctate, also known as humbug, is an integral protein of the endoplasmic reticulum and a truncated version of the aspartyl- β -hydroxylase, without the catalytic domain⁷⁹. Ubiquitously expressed, junctate interacts with stromal interaction molecule proteins to mediate store-operated Ca²⁺ entry in phagocytes, and was recently shown to mediate an alternative mechanism for releasing Ca²⁺ into phagosomes, thus playing an important role in maintaining Ca²⁺ homeostasis and increasing phagocytic efficiency⁸⁴. Both circASPH-1 and circASPH-2 are

backspliced from region encoding the transmembrane region, which is present in all ASPH transcripts.

1.5 Hypothesis Statement

Based on our previous RNAseq data of PBMCs from sepsis patients, as well as the critical role macrophages play in orchestrating immune responses, I hypothesize that circASPH plays a crucial role in the regulation of macrophage polarization in sepsis and overexpression of circASPH promotes an M1 response. I aim to test these hypotheses through two aims: 1) Determine circASPH expression profiles in macrophages in response to polarization stimuli, and; 2) Investigate the effect of circASPH knockdown on macrophage M1 polarization.

Chapter 2

2 Materials and Methods

2.1 Septic PBMC sample collection

Peripheral blood samples were collected from 8 sepsis patients at ICU-AD and ICU-DC at London Health Sciences Centre. Written consent forms were collected from all participants. The study was approved by Lawson Health Research Institute and the Western University Research Ethics Board and followed the guidelines of the Canadian Institutes of Health Research. Patient demographic and clinical information is presented in Table S1.

For PBMC isolation, whole blood in ethylenediaminetetraacetic acid (EDTA) tubes were centrifuged at 760 g for 10 min, and plasma was collected. The remaining blood cells were diluted 1:1 with phosphate-buffered saline (PBS; Gibco, Grand Island, NY, USA; Cat. no. 10010-023) and 7 mL of diluted blood cells were carefully overlaid on 4 mL of Ficoll-Paque™ PLUS (Cytiva, Mississauga, ON; Cat. no. 17144002). After centrifugation at 1,000 g for 25 min with minimal acceleration and without breaking, PBMCs between the plasma and Ficoll layers were carefully collected and washed twice with PBS.

2.2 Total RNA extraction

Total RNA was isolated using the standard TRIzol method. Briefly, 1 mL QIAzol™ Lysis Reagent (Qiagen, Toronto, ON; Cat. no. 79306) was added to cells and incubated at room temperature (RT) for 5 min. A 1:5 volume, or 200 µL, of chloroform (Bio Basic, Markham, ON; Cat. no. CC3000) was added, mixed thoroughly, and incubated again at RT for 5 min. After centrifugation for 15 min at 14,000 g and 4°C, the aqueous top layer

was carefully extracted and mixed with equal volume isopropanol (Bio Basic, Cat. no. IB0913). The mixture was incubated at RT for 10 min prior to centrifugation for 10 min at 14,000 g and 4°C. The supernatant was removed, and the pellet was washed twice by adding 1 mL cold 75% ethanol, and centrifuging for 5 min at 14,000 g and 4°C. The pellet was dried for 30 min at RT prior to resuspension in 20 µL RNase Free H₂O and heated for 10 min at 55°C. RNA concentration was measured using a nanodrop (NanoDrop, Wilmington, DE, USA).

2.3 cDNA synthesis

Complementary DNA (cDNA) was synthesized from total RNA using OneScript® Plus cDNA Synthesis Kit (Applied Biological Materials Inc., Richmond, BC; Cat. no. G236) according to manufacturer's protocol. Briefly, 2 µg total RNA was loaded into a reaction of 15 µL with 500 nM random primers, 500 µM dNTPs, and 100 nM circASPH-1 reverse primer listed in Table 2.1, then incubated at 65°C for 5 min before cooling on ice for 2 min. Reverse transcription (RT) buffer and 1 µL Reverse transcriptase were then added up to 20 µL, and the mixture was incubated 25°C for 10 min, 55°C for 15 min, then 85°C for 5 min in a T100 thermal cycler (Bio-Rad Laboratories Ltd., Mississauga, ON, Canada).

2.4 Quantitative Polymerase Chain Reaction (qPCR)

Primers were designed and ordered from Invitrogen (Burlington, ON). Primer information can be found in Table 2.1. Quantitative PCR (qPCR) was performed using BlastTaq™ 2x qPCR master mix (Applied Biological Materials; Cat. no. G892) with 300 nM primers and 2 µL of 1:10 diluted cDNA. Samples were heat-shocked at 95°C for 3

min, followed by 40 cycles of 95°C for 5 s, 60°C for 10 s, and 72 °C for 10s in a QuantStudio™ 3 Real-Time PCR System (Thermo Fischer Scientific). Relative gene expression was calculated using the $2^{-\Delta\Delta C_t}$ method with 18S as the loading control.

Table 2.1 Primer sequences used for qPCR

Target	Sequence	Amplicon Size (bp)
18S	F: 5'-TGGTGGAGCGATTTGTCTGG	118
	R: 5'-GAACGCCACTTGTCCCTCTA	
ASPH	F: 5'-CTTCAGAGCCAGCAGTCCC	173, 302
	R: 5'-CACGTGGTAACTATGCTCGGT	
circASPH-1	F: 5'-TGAGGAAGTTCTAGGAAAAGTAGG	214
	R: 5'-AACAAGATCAAACCAAACGACAGC	
circASPH-2	F: 5'-GCCAAAGCAAAGGACTTCCG	195
	R: 5'-GACGCCCAGCAATGCAATC	
IL-1b	F: 5'-AGCTACGAATCTCCGACCAC	133
	R: 5'-AAGGTGCTCAGGTCATTCTCC	
TNFa	F: 5'-CCCATCTATCTGGGAGGGGT	113
	R: 5'-ATCCCAAAGTAGACCTGCCC	
IL-6	F: 5'-GATTCAAAGATGTAGCCGCC	150
	R: 5'-TGCCTCTTTGCTGCTTTTCAC	
CXCL9	F: 5'-ACCGCTATCATTCAAAGGAGG	178
	R: 5'-TCAACTGGTGGGTGGTAGAAG	
STAT1	F: 5'-AAAGCAAGACTGGGAGCACG	189
	R: 5'-GACATCTGGATTGGGTCTTCCT	
ALOX15	F: 5'-GGCTGGGGCCAAACTATATGA	183
	R: 5'-TTGCTCTGACCACACCAGAAA	
CCL17	F: 5'-TTCGGACCCCAACAACAAGA	190
	R: 5'-GCTCTTCTTCGTCCCTGGAA	

PCR products were separated on 1.5% agarose (Amresco, Solon, OH, USA; Cat. no. 0710-500G) gels in Tris-acetate-EDTA buffer (40 mM Tris base, 20 mM acetic acid, and 1 mM EDTA) and SYBR™ Safe DNA gel stain (Invitrogen, Cat. no. S33102). Bands were visualized using a FluorChem M system (ProteinSimple, San Jose, CA, USA).

2.5 Cell culture

THP-1 cells from the American Type Culture Collection (ATCC; Manassas, VA, USA; TIB-202) were maintained in ATCC-modified Roswell Park Memorial Institute-1640 medium (RPMI-1640; Gibco, Cat. no. A10491-01) supplemented with 10% fetal bovine serum (FBS; Gibco, Cat. no. 16140071) and 5 nM β -mercaptoethanol (Sigma, St. Louis, MO, USA; Cat. no. M6250) according to ATCC guidelines. Cells were cultured in a humidified incubator at 37 °C with 5% CO₂.

2.5.1 THP-1 model of macrophage polarization

Prior to downstream experiments, THP-1 cells were plated at 500,000 cells/well in a 12-well plate and differentiated to macrophages by culturing in 25 ng/mL (40.6 nM) phorbol 12-myristate 13-acetate (PMA; Sigma, Cat. no. 19-144) for 48 h, then rested in PMA-free complete medium for 24 h. The rest period length was determined empirically by assessing IL-1 β expression in the cells after PMA removal. THP-1 macrophages were then stimulated towards an M1 phenotype with 20 ng/mL IFN- γ (PreproTech, Cranbury, NJ, USA; Cat. no. 300-02) and 5 ng/mL LPS from *E.coli* O111:B4 (MilliporeSigma, Burlington, MA, USA; Cat. no. L2630) or stimulated towards an M2 phenotype with 30 ng/mL IL-4 (PreproTech, Cat. no. 200-04) for up to 48 h prior to harvesting.

2.6 RNA-Fluorescence in situ Hybridization

THP-1 cells were differentiated with PMA, rested in PMA-free complete medium, and were either untreated or polarized with IFN- γ + LPS for 24 h or IL-4 for 12 h as described above. These time points were chosen to validate the overexpression of circASPH found by qPCR. The medium was removed, and the cells were washed with 1

mL cold PBS and fixed with 3.7% formaldehyde solution (LabChem, Zelienople, PA, USA; Cat. no. LC146704) for 30 min at 4°C. Cells were washed with 1 mL cold PBS for 2 min before permeabilization with 500 µL PBS with 0.25% Triton X-100. Cells were again washed with 1 mL cold PBS for 2 min and incubated for 30 min at 37°C in pre-hybridization buffer (Table 2.2). Cells were then hybridized at 37°C overnight in 300 µL pre-hybridization buffer with 500 nM cyanine-5 (Cy5)-conjugated circASPH probe (5'-Cy5-GTCCTCCATGCTTTGTCTCTAATAAAACTTTGGCATCA, Sigma-Aldrich) or random probe (5'-Cy5-CAATGGCAAGGACGAGCGATCTATGCCCCGTACGCGGA, Sigma-Aldrich). Cells were washed in 2 mL 2x SSC (Table 2.3) in a 32°C water bath for 15 min with the shaker set to 40 rpm, followed by a second wash in the same condition and duration with 1 mL PBS containing 0.1% Tween® 20 (PBS-T; Sigma-Aldrich, Cat. no. P1379). Cells were stained with 500 µL PBS containing 1:10000 4',6-diamidino-2-phenylindole (DAPI) for 5 min at RT, then washed with 1 mL PBS-T. Cells were then imaged using a Nikon Eclipse Ts2 inverted microscope (Nikon, Mississauga, ON).

Table 2.2 Recipe for pre-hybridization buffer for RNA-FISH

Component	Company	Cat. no.	Concentration
Formamide	Sigma-Aldrich	F9037	10%
Dextran sulfate	Thermo Scientific	441490050	100 mg/mL
Bovine serum albumin (BSA)	Amresco	0332	100 µg/mL
Saline sodium citrate buffer (SSC)	Homemade (Table 2.3)		5x
RNaseOUT™	Life Technologies	100000840	40 U/mL

Table 2.3 Recipe for 5x saline sodium citrate buffer

Component	Concentration
Sodium Chloride (NaCl)	750 mM
Sodium Citrate	75 mM
Hydrochloric Acid (HCl)	As required to adjust pH to 7.0

2.7 Transfection

THP-1 cells were differentiated with PMA and rested in PMA-free complete medium as described above. Cells were transfected with siRNA and Endofectin™ Max (GeneCopoeia, Rockville, MD, USA; Cat. no. EF013) according to the manufacturer's protocol. Briefly, 2 μ L Endofectin™ Max and 1 μ g anti-circASPH siRNA (si-circASPH; 5'-AGUUUUAUUAGAGACAAA-3', Sigma-Aldrich) or NC siRNA (5'-CGUACGCGGAAUACUUCGA-3', Sigma-Aldrich) were each diluted in 50 μ L Opti-MEM (Gibco, Cat. no. 31985-062). After 5 min of incubation at RT, the siRNA and Endofectin mixtures were combined, thoroughly mixed, and incubated for 15 min at RT. Cells were cultured in 400 μ L complete media, and the 100 μ L siRNA-Endofectin mixtures were added at 37°C. After 6 h, 500 μ L of complete medium was added and cells were stimulated with IFN- γ + LPS or IL-4 for 24 h, as this is the first time point where both isoforms of circASPH, as well as all M1 and M2 gene markers were determined to be significantly induced, and to ensure consistency between M1 and M2 experiments.

2.8 Cell death assay

Cell death was dynamically monitored during M1 polarization and transfection using a Cytation 5 Cell Imaging Multimode Reader (BioTek Instruments, Winooski, VM, USA) connected to a BioSpa 8 Automated Incubator (BioTek). Briefly, THP-1 cells were

differentiated, transfected, and stimulated with IFN- γ + LPS as described above. Cells were placed into the BioSpa immediately after transfection, with 1 $\mu\text{g}/\text{mL}$ propidium iodide (PI, Thermo Fisher Scientific, Cat. no. P3566) added to each well. The plate was automatically transferred to the Cytation 5 every two hours, and eight images of high contrast bright field and Texas Red (excitation: 586 nm; emission: 647 nm) fluorescence were taken per well at 4x magnification. PI-stained cells represented by red objects were automatically counted by the BioTek software Gen5, and total cells were counted from the bright field images using the Analyze Particles function in ImageJ⁸⁵. Both counts were summed across the eight images taken at each time point, and the proportion of PI-positive cells was calculated and plotted against time.

2.9 Western blotting

Transfected THP-1 cells stimulated with IFN- γ + LPS for 24 h were collected by scraping and centrifuged at 300 g for 5 min at 4°C. The supernatant was removed, and the pellet was resuspended in 75 μL cold RIPA lysis buffer (Cell Signaling Technology, Danvers, MA, USA; Cat. no. 9806) supplemented with 1 mM phenylmethanesulfonyl fluoride (PMSF; Cell Signaling, Cat. no. 8553S) and incubated on ice for 20 min. After centrifugation at 14,000 g for 20 min, the supernatant was collected, and protein concentration was measured using a Pierce™ BCA protein assay (Thermo Fisher Scientific, Cat. no. 23225) with a standard curve generated by bovine serum albumin (BSA; Amresco, Cat. no. 0332). Proteins were diluted to 0.8 $\mu\text{g}/\mu\text{L}$ in Laemmli loading buffer containing 65.8 mM Tris-HCl, pH 6.8, 26.3% (w/v) glycerol, 2.1% SDS, 0.01% Bromophenol blue, and 5% β -mercaptoethanol. Samples were boiled at 95°C for 5 min, then 20 μg of protein were loaded per well and run on a 10% polyacrylamide SDS gel at

60 V for 30 min followed by 100 V for 90 min. Proteins were transferred onto polyvinylidene fluoride membranes using the Trans-Blot TURBO Transfer System (Bio-Rad, Hercules, California, USA) according to manufacturer's protocol. Blocking was done in PBS-T containing 5% skim milk powder (BioShop, Burlington, ON; Cat. no. SKI400.250) for 1 h, then membranes were incubated with primary antibody diluted 1:3000 in PBS-T at 4°C overnight. Primary antibodies used are listed in Table 2.4. After 3 washes for 10 min each in PBS-T, membranes were incubated with either donkey anti-rabbit (Invitrogen, Cat. no. A16023) or goat anti-mouse (Invitrogen, Cat. no. A16066) secondary antibody diluted 1:4000 in PBS-T at RT for 1 h. After another 3 washes for 15 min each in PBS-T, membranes were developed using Clarity™ Western ECL Substrate (Bio-rad, Cat. no. 1705060) or Clarity™ Max Western ECL Substrate (Bio-rad, Cat. no. 1705062) for protein bands with weaker signal. Membranes were imaged using a FluoroChem M (Protein Simple). Protein bands were visualized with chemiluminescence and protein markers with red fluorescence. To re-blot with a different primary antibody, membranes were washed in PBS for 10 min and stripped using mild stripping buffer (200 mM glycine, 0.1% SDS, 1% Tween® 20, adjusted to pH 2.2) twice for 15 min each. Membranes were then washed in PBS-T 3 times for 10 min each before blocking and immunoblotting as described above. Densitometry analysis was performed in ImageJ. Briefly, chemiluminescent intensity of protein bands was quantified by the mean gray value in a rectangular region of interest around each band, with all regions of interest for the same protein being the same size. The intensity measurement was adjusted by subtracting background intensity and normalized to β -actin of the same sample. Expression for phosphorylated proteins were further normalized to their total expression.

Table 2.4 List of primary antibodies used for western blotting

Target	Company (cat. no)	Host species
NF- κ B p65	Cell signaling (6956)	mouse
p-NF- κ B p65	Cell signaling (3033)	rabbit
STAT1	Cell signaling (14995)	rabbit
p-STAT1	Cell signaling (9167)	rabbit
β -actin	Santa Cruz (sc-47778)	mouse

2.10 Multiplex cytokine assay

Blood plasma collected from sepsis patients at ICU-AD and ICU-DC, as well as cell culture medium from THP-1 cells that were differentiated, transfected, and stimulated with IFN- γ + LPS for 24 h as described above, were centrifuged at 500 g for 5 min to remove debris. Plasma samples were diluted 1:1 with PBS. Samples were sent to Eve Technologies (Calgary, AB) and analyzed using their Human Cytokine Proinflammatory Focused 15-Plex Discovery Assay® Array (MilliporeSigma, Cat. no. HDF15) according to the manufacturer's protocol. The assay uses the Luminex™ 200 system (Luminex, Austin, TX, USA) to simultaneously measure 15 targets consisting of GM-CSF, IFN- γ , IL-1 β , IL-1Ra, IL-2, IL-4, IL-5, IL-6, IL-8, IL-10, IL-12p40, IL-12p70, IL-13, MCP-1, and TNF- α . Assay sensitivities range from 0.14-5.39 pg/mL for these targets.

2.11 Statistical analysis

The student's t-test and one-way ANOVA followed by Dunnett's multiple comparisons test were conducted for comparison between two groups or three or more groups, respectively. The ratio paired t-test was used where indicated. Correlation between

circASPH and cytokine levels was analyzed using linear regression. All statistical tests were performed in GraphPad Prism 9. Statistical significance was defined as $p < 0.05$.

Chapter 3

3 Results

3.1 CircASPH is overexpressed in PBMCs at ICU admission

Our previous RNAseq found that circASPH was upregulated in PBMCs collected at ICU-AD compared with those collected at ICU-DC. To validate the overexpression of circASPH in septic PBMCs at ICU-AD, quantitative reverse transcription PCR (qRT-PCR) was performed. PBMCs were isolated from blood samples collected from 6 sepsis patients at ICU-AD and ICU-DC. Total RNA was extracted, and circASPH expression was quantified by qRT-PCR using primers listed in Table 2.1. To validate PCR specificity, PCR products were run and separated using gel electrophoresis. There was only one unique band observed with the predicted size for each pair of primers used (Fig. S1). Both isoforms of circASPH were significantly overexpressed in PBMCs collected at ICU-AD compared with those collected at ICU-DC (Fig. 3.1).

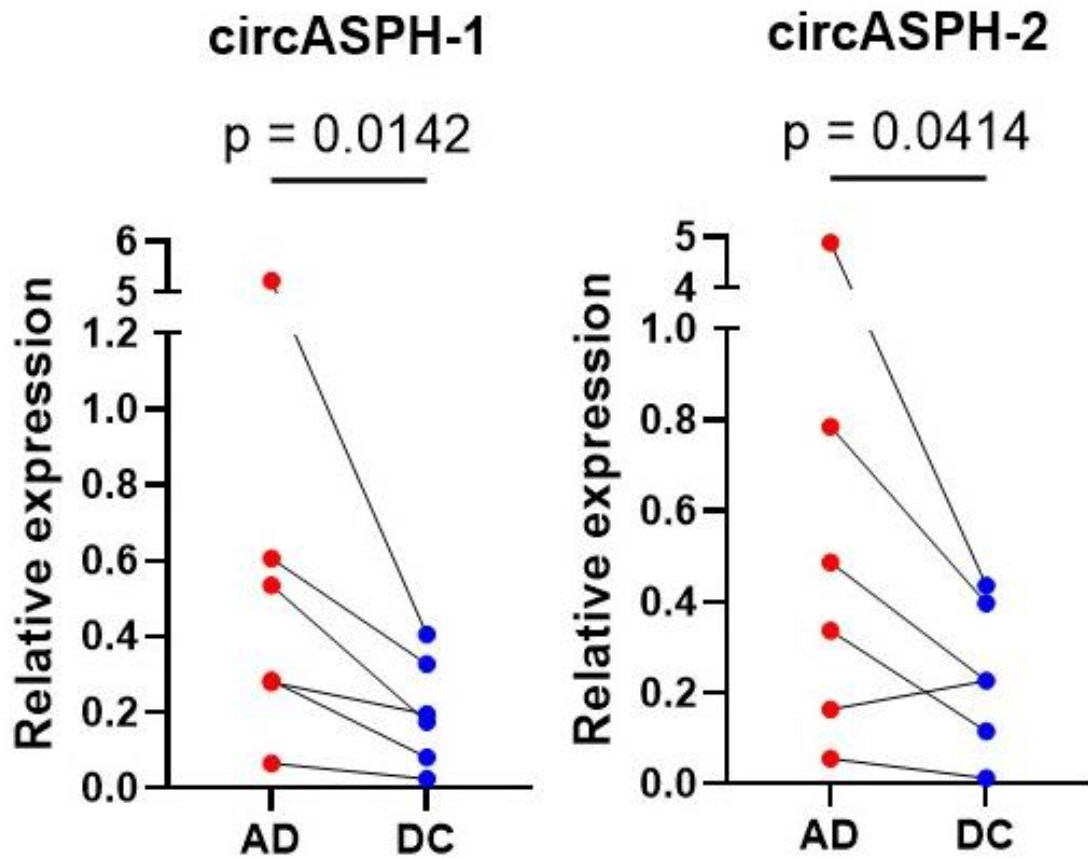


Figure 3.1 CircASPH overexpressed in septic PBMCs before intensive care. PBMCs were collected from sepsis patients at ICU admission (AD) and discharge (DC). Total RNA was isolated, cDNA synthesized, and relative expression of both isoforms of circASPH were quantified with qPCR using the $2^{-\Delta\Delta C_t}$ method, with 18S as internal control. Data belonging to the same patient were joined with a line (n = 6). P-values calculated from paired ratio t-test.

3.2 CircASPH expression level in septic PBMCs correlates with plasma cytokine levels of IL-12p70 and IL-5

To explore possible correlations between circASPH expression in PBMCs and blood cytokine levels in sepsis patients, plasma collected from 8 sepsis patients at ICU-AD and ICU-DC were sent to be analyzed by a multiplex immunoassay including 15 cytokines (GM-CSF, IFN- γ , IL-1 β , IL-1Ra, IL-2, IL-4, IL-5, IL-6, IL-8, IL-10, IL-12p40, IL-12p70, IL-13, MCP-1, and TNF- α). Levels of GM-CSF, IL-1Ra, IL-2, IL-6, and IL-10 were significantly higher in plasma collected at ICU-AD, while the remaining cytokines did not significantly change, with the increase of TNF- α approaching significance (Fig. 3.2). The correlation between circASPH expression and plasma cytokine levels at ICU-AD and ICU-DC was also analyzed. Expression levels for both isoforms of circASPH were found to correlate to levels of the heterodimeric form of IL-12, IL-12p70, at ICU-AD and to IL-5 levels at ICU-DC (Table 3.1, Fig. 3.3). The remaining cytokines were not significantly correlated with circASPH levels (Table 3.1). One patient was excluded from the correlation analysis for ICU-DC as they had undetectable circASPH expression at ICU-DC.

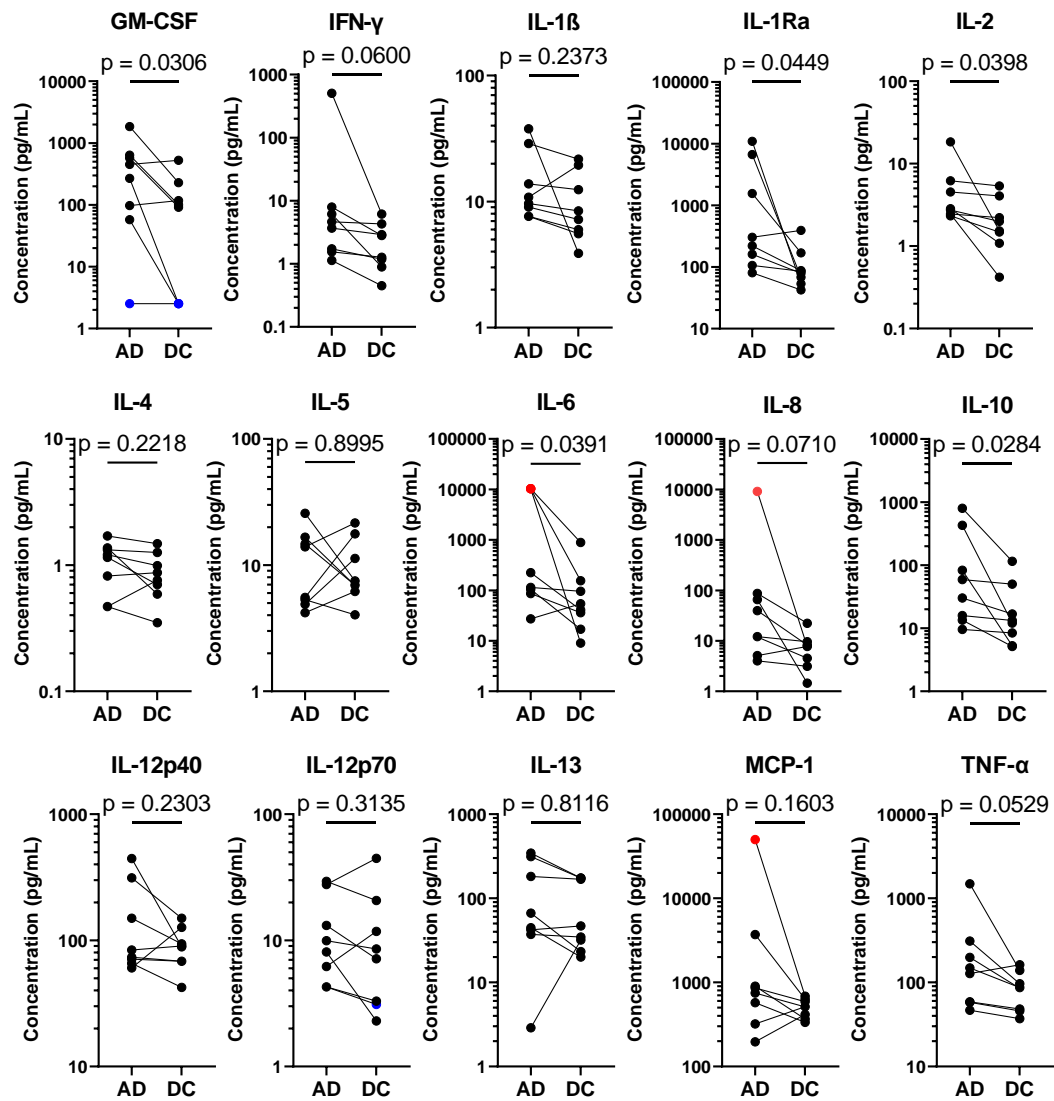


Figure 3.2 Overexpression of cytokines in sepsis patients at the start of intensive care. Blood plasma was collected from sepsis patients at ICU admission (AD) and discharge (DC) using EDTA tubes, and cytokine concentrations were quantified by multiplex cytokine immunoassay (n = 8). Red or blue data points indicate values out of range above or below the standard curve, and were assigned the highest or lowest standard value, respectively. P-values calculated from paired ratio t-test.

Table 3.1 Correlation results between circASPH and plasma cytokine levels before and after intensive care

Cytokine	ICU-AD ^a				ICU-DC ^a			
	circASPH-1		circASPH-2		circASPH-1		circASPH-2	
	r ²	p	r ²	p	r ²	p	r ²	p
GM-CSF	0.0354	0.6862	0.023	0.7454	0.0153	0.8155	0.0299	0.7432
IFN- γ	0.2595	0.2429	0.0944	0.5027	0.2649	0.2961	0.2837	0.2766
IL-1 β	0.1637	0.3679	0.2617	0.2406	0.0016	0.9396	0.0002	0.9808
IL-1Ra	0.2342	0.2711	0.0921	0.5082	0.1013	0.5387	0.0804	0.586
IL-2	0.0728	0.5584	0.0818	0.5342	0.0065	0.8797	0.0154	0.8148
IL-4	0.2126	0.2977	0.1873	0.3321	0.2236	0.3436	0.2665	0.2945
IL-5	0.1093	0.4689	0.1036	0.4815	0.7552	0.0246	0.7925	0.0174
IL-6	0.163	0.369	0.0681	0.5718	0.0807	0.5854	0.0976	0.5466
IL-8	0.0024	0.9172	0.0032	0.9041	0.233	0.3322	0.2214	0.3463
IL-10	0.3019	0.2014	0.1323	0.4225	0.0202	0.788	0.0276	0.753
IL-12p40	0.3713	0.1464	0.0834	0.53	0.3058	0.2551	0.3175	0.2443
IL-12p70	0.8846	0.0016	0.7415	0.0128	0.0833	0.5791	0.0942	0.5541
IL-13	0.5422	0.0591	0.1538	0.3842	0.0281	0.7511	0.0539	0.658
MCP-1	0.2463	0.2572	0.0869	0.521	0.4998	0.1162	0.4918	0.1205
TNF- α	0.3322	0.1756	0.1349	0.4177	0.146	0.4547	0.1696	0.4172

^a r² and p-values were calculated using simple linear regression

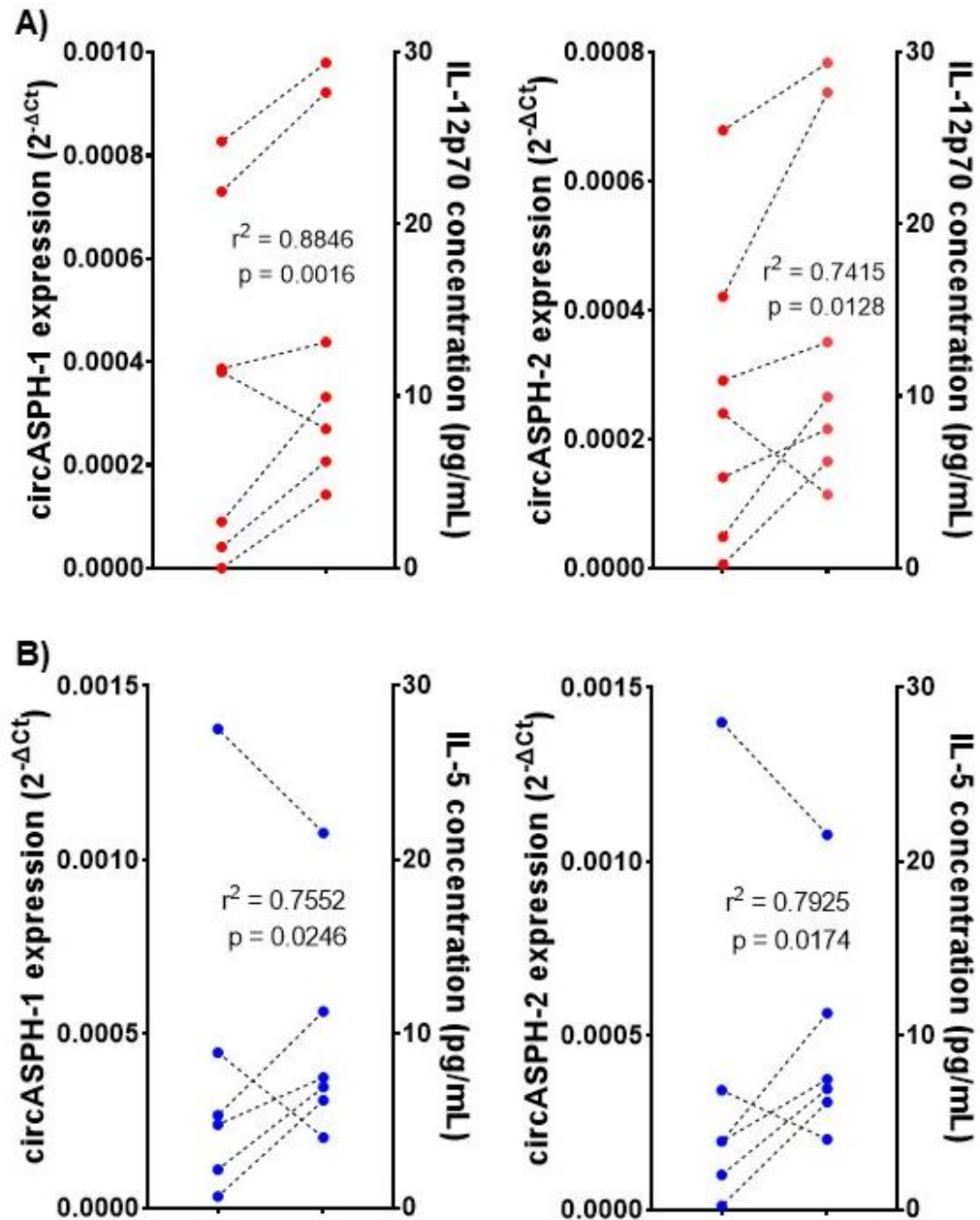


Figure 3.3 CircASPH correlates with IL-12 at ICU-AD and IL-5 at ICU-DC. PBMCs and blood plasma were collected from sepsis patients at ICU admission (AD) and discharge (DC). Total RNA was isolated from PBMCs, cDNA synthesized, and relative expression of both isoforms of circASPH were quantified with qPCR using the $2^{-\Delta\Delta Ct}$ method, with 18S as internal control. Plasma cytokine concentrations were quantified by multiplex cytokine immunoassay. Correlation of circASPH-1 (left) and circASPH-2 (right) expression to IL-12p70 at AD (**A**, $n = 7$) and to IL-5 at DC (**B**, $n = 6$). Dotted lines join data from the same patient. R^2 and p -values were calculated using linear regression.

3.3 PMA induces IL-1 β expression during differentiation of THP-1 macrophages

PMA is commonly used to differentiate THP-1 monocytes into macrophages³⁵; however, PMA slightly activates M1 genes and hinders M2 polarization. Baxter and colleagues showed that allowing THP-1 cells to rest in PMA-free medium before cytokine stimulation improves M2 differentiation³⁸. To select the optimal time for THP-1 cells to rest in PMA-free media prior to cytokine stimulation, THP-1 cells were differentiated with 25 ng/mL PMA for 48 h and cultured in PMA-free medium for 0, 1, or 2 d before harvesting (Figure 3.4A). Total RNA was collected, cDNA was synthesized, and expression of IL-1 β , an M1 effector gene, was quantified through qPCR as an indicator of macrophage activation. PCR product lengths were validated using gel electrophoresis (Figs. S1, S2). IL-1 β expression was significantly elevated after PMA treatment, but returned to a level similar to monocytes 24 h after removal of PMA, suggesting that the cell has returned to a resting state (Fig. 3.4B). As such, PMA-differentiated THP-1 cells were rested in PMA-free media for 24 h prior to downstream experiments.

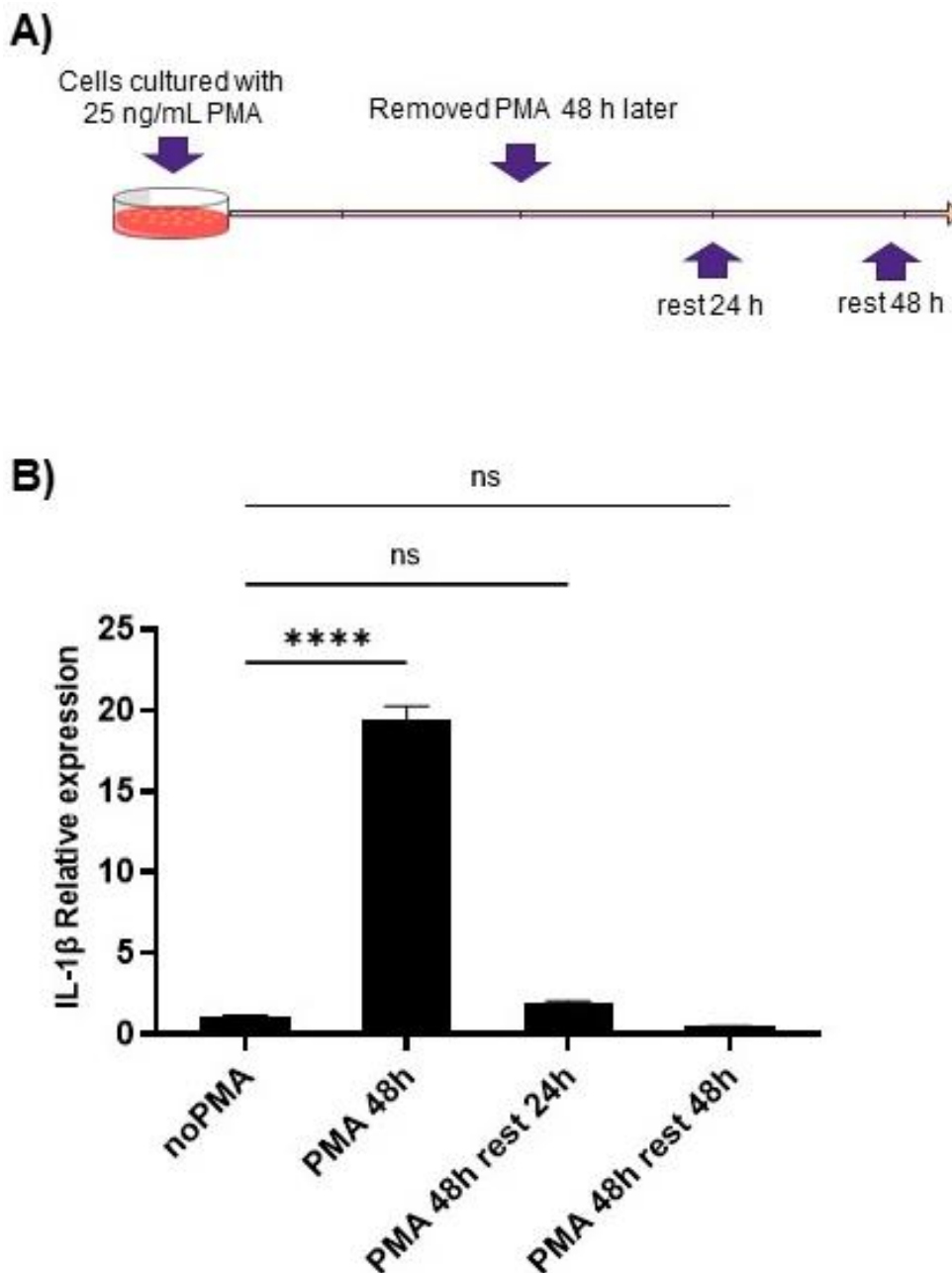


Figure 3.4 PMA induces IL-1 β expression during THP-1 differentiation. (A) Schematic of PMA stimulation and removal during experiment. THP-1 cells were harvested as monocytes (noPMA), differentiated with 25 ng/mL PMA for 48 h and harvested (PMA), or differentiated with 25 ng/mL PMA for 48 h and rested in PMA-free media for 1 or 2 d. Total RNA was harvested and cDNA was synthesized. (B) Relative expression of IL-1 β quantified through qPCR using the $2^{-\Delta\Delta C_t}$ method, with 18S as an internal control. Data presented as mean \pm SEM (n = 3). ****, p < 0.001 by one-way ANOVA followed by Dunnett's multiple comparisons test.

3.4 Alteration in expression of circASPH isoforms between THP-1 monocytes and macrophages

To quantify the baseline circASPH expression profile during the initial differentiation stage, cDNA generated in the previous section were used to quantify expression for circASPH isoforms 1 and 2, and linear ASPH through qPCR. CircASPH-1 was downregulated by 2 d after PMA removal, and circASPH-2 was upregulated by 1 d after PMA-removal compared with THP-1 monocytes (Fig. 3.5). Linear ASPH expression was unchanged throughout the differentiation and resting process (Fig. 3.5)

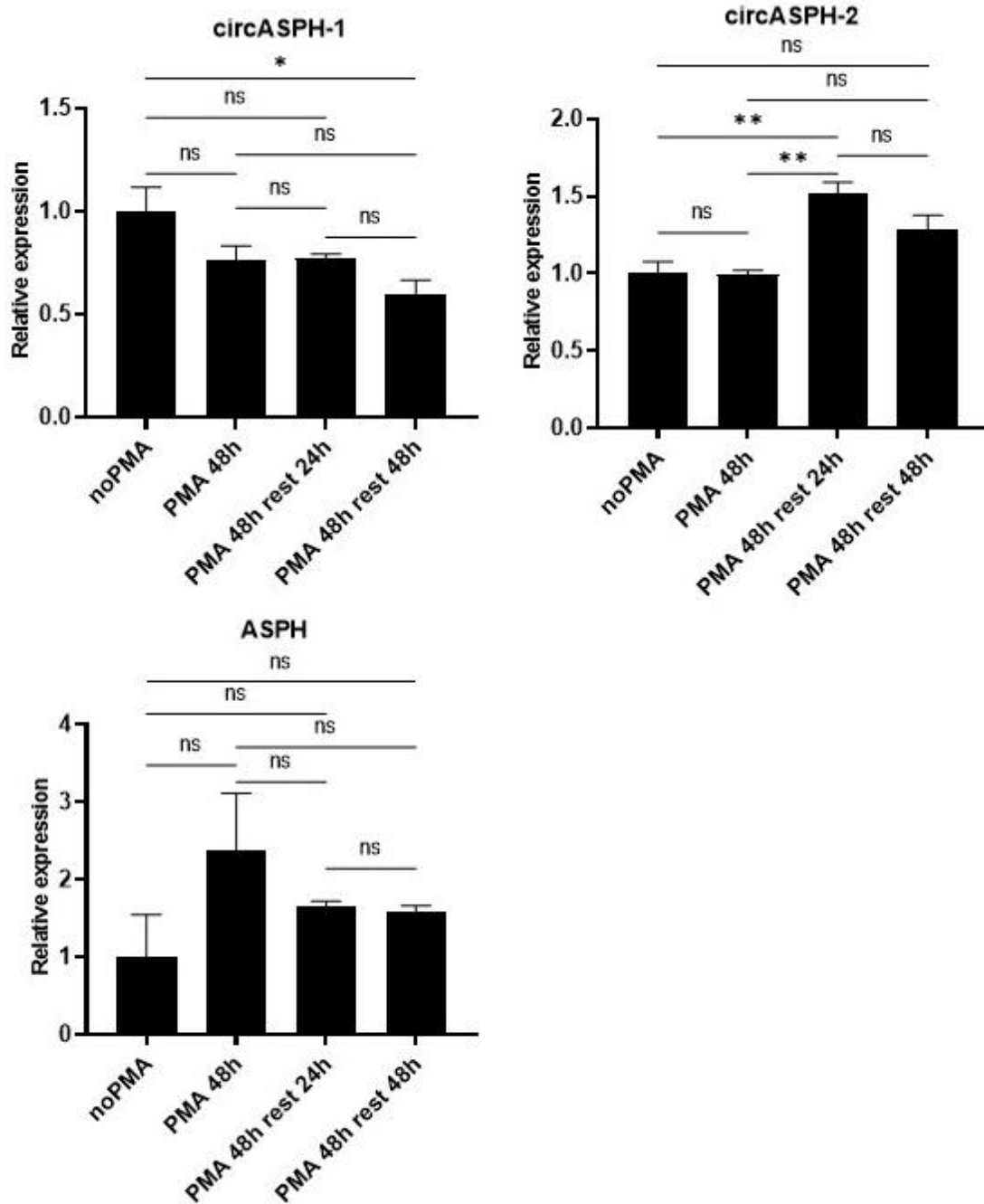


Figure 3.5 PMA removal alters circASP expression. THP-1 cells were harvested as monocytes (noPMA), differentiated with 25 ng/mL PMA for 48 h and harvested (PMA 48h), or differentiated with 25 ng/mL PMA for 48 h and rested in PMA-free media for 24 or 48 h. Total RNA was harvested, cDNA was synthesized, and relative expression of circASP isoforms and ASPH were quantified through qPCR using the $2^{-\Delta\Delta C_t}$ method, with 18S as an internal control. Data presented as mean \pm SEM (n = 3). *, p < 0.05; **, p < 0.01 by one-way ANOVA followed by Dunnett's multiple comparisons test.

3.5 Validation of macrophage polarization model

To validate the *in vitro* model of macrophage polarization, and to characterize the expression of macrophage polarization gene markers during cytokine stimulation, THP-1 cells were differentiated and rested as described above, then stimulated with IFN- γ + LPS or IL-4 for up to 2 d. Effectiveness of polarization was measured by the expression of M1 gene markers (IL-1 β , TNF- α , IL-6, CXCL9, and STAT1) or M2 gene markers (ALOX15 and CCL17), quantified through qRT-PCR. PCR product specificities were validated using gel electrophoresis (Figs. S1, S2). Expression of M1 cytokines IL-1 β , TNF- α , IL-6, and CXCL9 sharply peaked at 6 h of stimulation, while expression of the transcription factor STAT1 was significantly elevated at 6 h but continued to rise even after 2 d (Fig. 3.6A). In contrast, expression of M2 cytokine CCL17 peaked only after 1 d, while expression of the enzyme ALOX15 became significantly elevated at 1 d and continued to rise after 2 d (Fig. 3.6B).

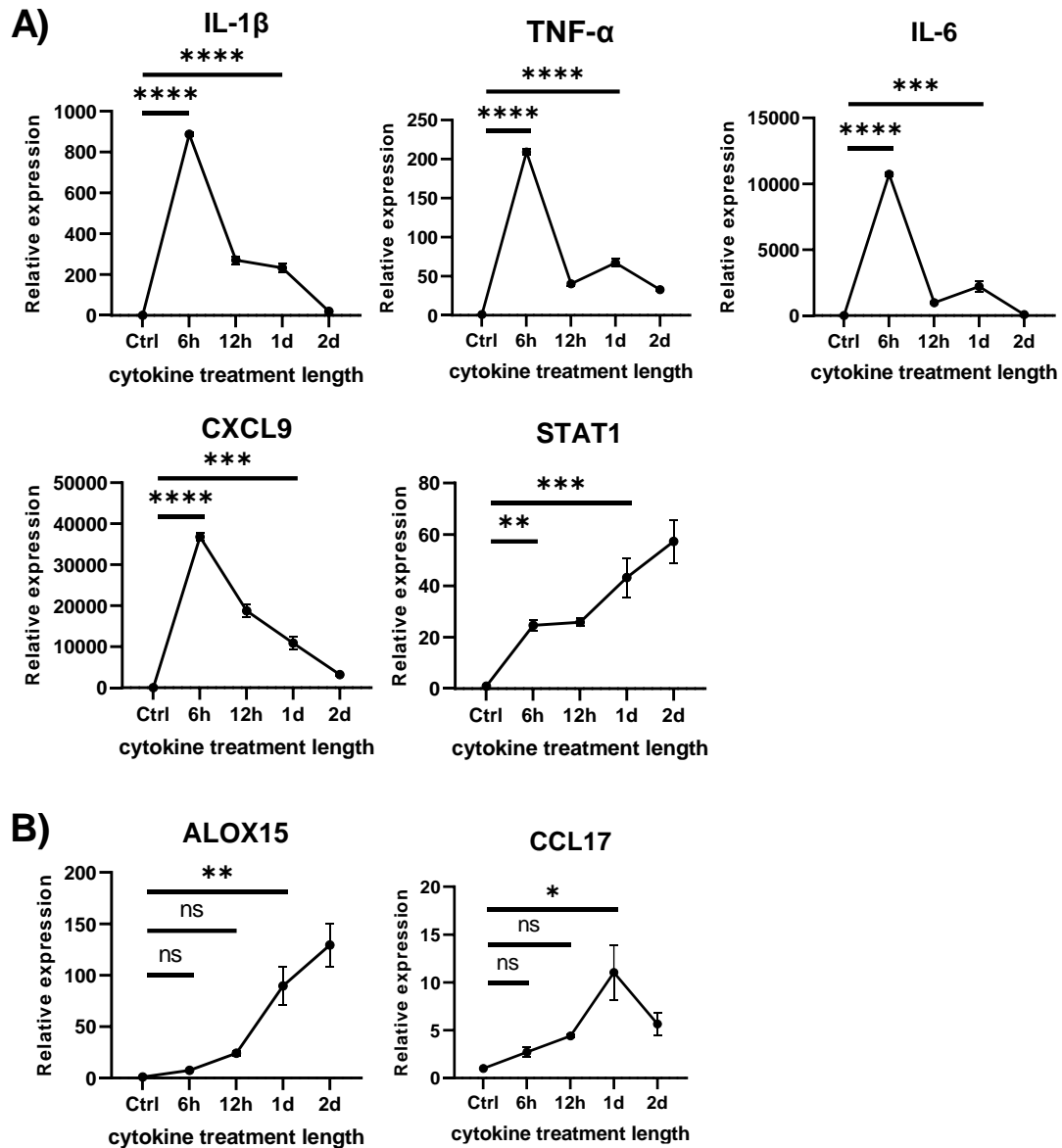


Figure 3.6 Cytokine stimulation induces THP-1 macrophage polarization gene markers. THP-1 cells were differentiated with 25 ng/mL PMA for 48 h and rested in PMA-free media for 24 h, then treated with 20 ng/mL IFN- γ + 5 ng/mL LPS or 30 ng/mL IL-4 for up to 2 d. Total RNA was harvested and cDNA was synthesized. Relative expression of M1 gene markers after IFN- γ + LPS stimulation (**A**) or M2 gene markers after IL-4 stimulation (**B**) were quantified through qPCR using the $2^{-\Delta\Delta C_t}$ method, with 18S as an internal control. Data presented as mean \pm SEM (n = 3). *, p < 0.05; **, p < 0.01; ***, p < 0.005; ****, p < 0.001 by one-way ANOVA followed by Dunnett's multiple comparisons test.

3.6 Alteration of circASPH and ASPH expression by cytokine stimulation

To quantify circASPH expression profile during M1 and M2 polarization, cDNA generated in the previous section were used to quantify expression for circASPH isoforms 1 and 2, and linear ASPH through qPCR. During IFN- γ + LPS stimulation, expression for both isoforms of circASPH peaked at 1 d; though surprisingly, linear ASPH expression was almost completely abolished at 6 h and 12 h before sharply peaking at 1 d as well (Fig. 3.7A). The backsplicing preference of circASPH was quantified by calculating the ratio between expression level of each circASPH isoform and that of the linear ASPH. The results showed that due to fluctuations in ASPH expression, the ratios of circASPH-1/ASPH and circASPH-2/ASPH significantly increased at 6 h and 12 h after stimulation, and then returned to baseline afterwards (Fig. 3.7B).

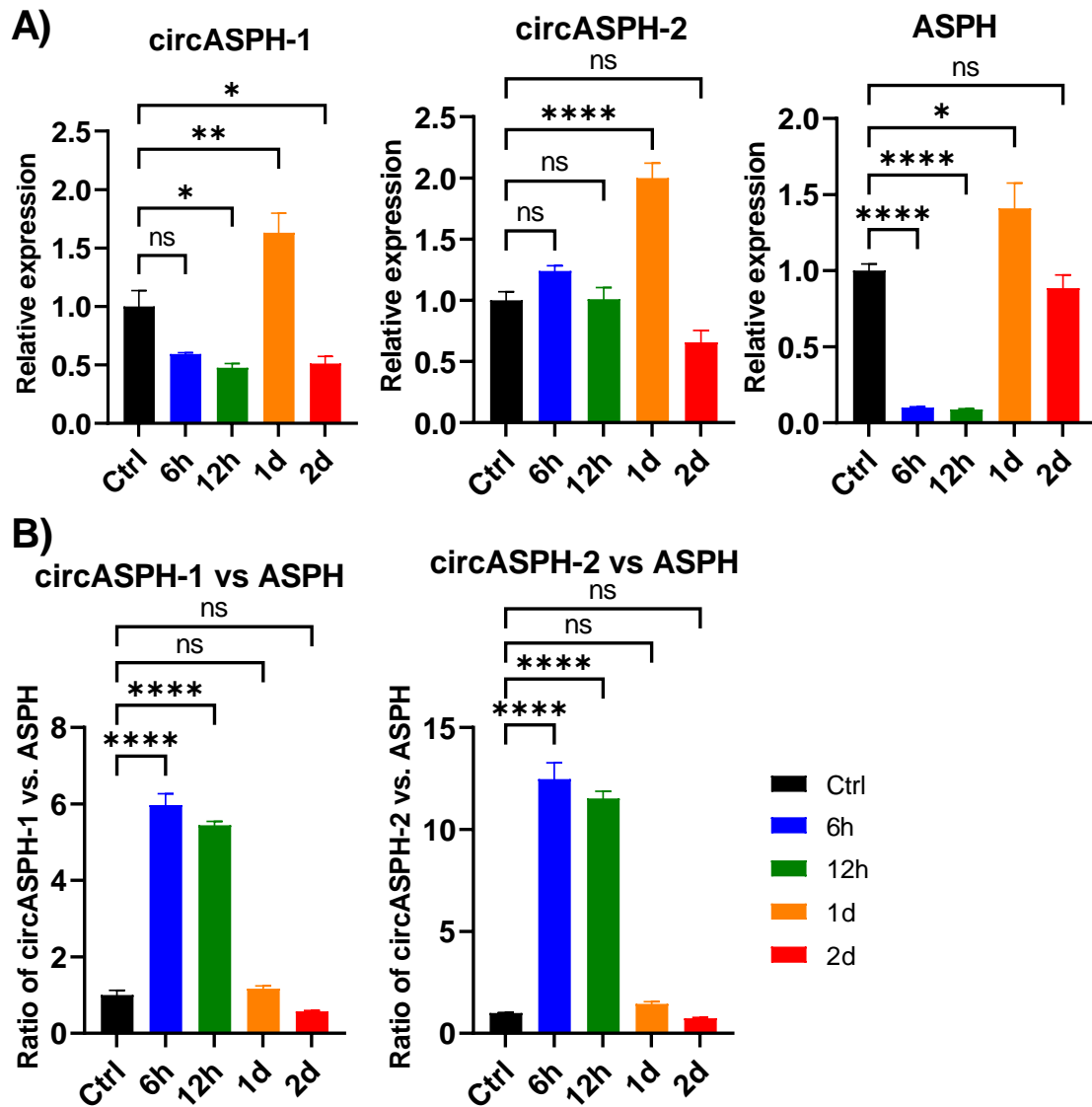


Figure 3.7 CircASPH and ASPH levels fluctuate during THP-1 macrophage M1 polarization. THP-1 cells were differentiated with 25 ng/mL PMA for 48 h and rested in PMA-free media for 24 h, then treated with 20 ng/mL IFN- γ + 5 ng/mL LPS for up to 2 d. Total RNA was harvested and cDNA was synthesized. **(A)** Relative expression of two isoforms of circASPH and linear ASPH, were quantified through qPCR using the $2^{-\Delta\Delta C_t}$ method, with 18S as an internal control. **(B)** Data from (A) represented as circASPH-to-ASPH expression ratios. All data represented as mean \pm SEM (n = 3). *, p < 0.05; **, p < 0.01; ****, p < 0.001 by one-way ANOVA followed by Dunnett's multiple comparisons test.

During IL-4 stimulation, expression for both isoforms of circASPH peaked at 12 h before dropping and becoming downregulated by 2 d; while linear ASPH expression continued rising and peaked at 1 d, remaining elevated at 2 d (Fig. 3.8A). Again, the circ-to-linear ratio was calculated to quantify splicing preference of circASPH. Results show that due to greater upregulation of ASPH, the ratios of circASPH-1/ASPH and circASPH-2/ASPH decreased at all detected time points compared with control cells, except for circASPH-2/ASPH at the 12 h time point (Fig. 3.8B).

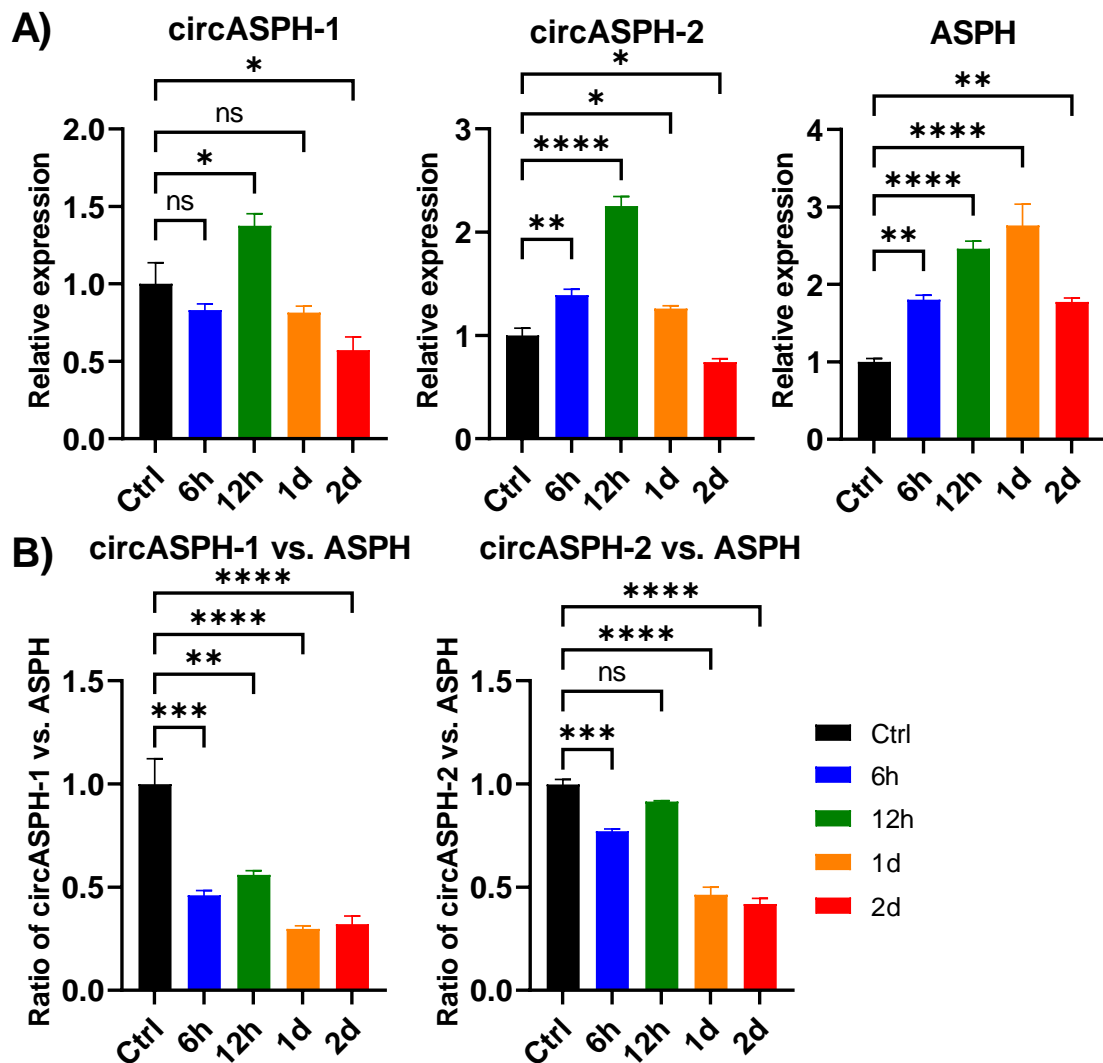


Figure 3.8 CircASP levels fluctuate while ASPH is elevated during THP-1 macrophage M2 polarization. THP-1 cells were differentiated with 25 ng/mL PMA for 48 h and rested in PMA-free media for 24 h, then treated with 30 ng/mL IL-4 for up to 2 d. Total RNA was harvested and cDNA was synthesized. **(A)** Relative expression of two isoforms of circASP and linear ASPH, were quantified through qPCR using the $2^{-\Delta\Delta Ct}$ method, with 18S as an internal control. **(B)** Data from (A) represented as circASP-to-ASPH expression ratios. All data represented as mean \pm SEM (n = 3). *, p < 0.05; **, p < 0.01; ***, p < 0.005; ****, p < 0.001 by one-way ANOVA followed by Dunnett's multiple comparisons test.

3.7 CircASPH is primarily localized in the cytoplasm

To determine cellular distribution of circASPH, RNA-fluorescent *in situ* hybridization (RNA-FISH) was performed on PMA-differentiated THP-1 cells using Cy5-labelled circASPH probes that are complementary to the circASPH BSJ sequence, or random probes which are not complementary to any sequence as a control. Cells were also stained with DAPI to visualize the nucleus. There was very strong red fluorescence seen in the cells hybridized with Cy5-circASPH (Fig. 3.9, top panel), whereas there was no red signal in the cells with random probes (Fig. 3.9, bottom panel). Qualitative analysis on the merged image of circASPH probe and DAPI signals suggests that circASPH is mainly expressed in the cytoplasm (Fig. 3.9).

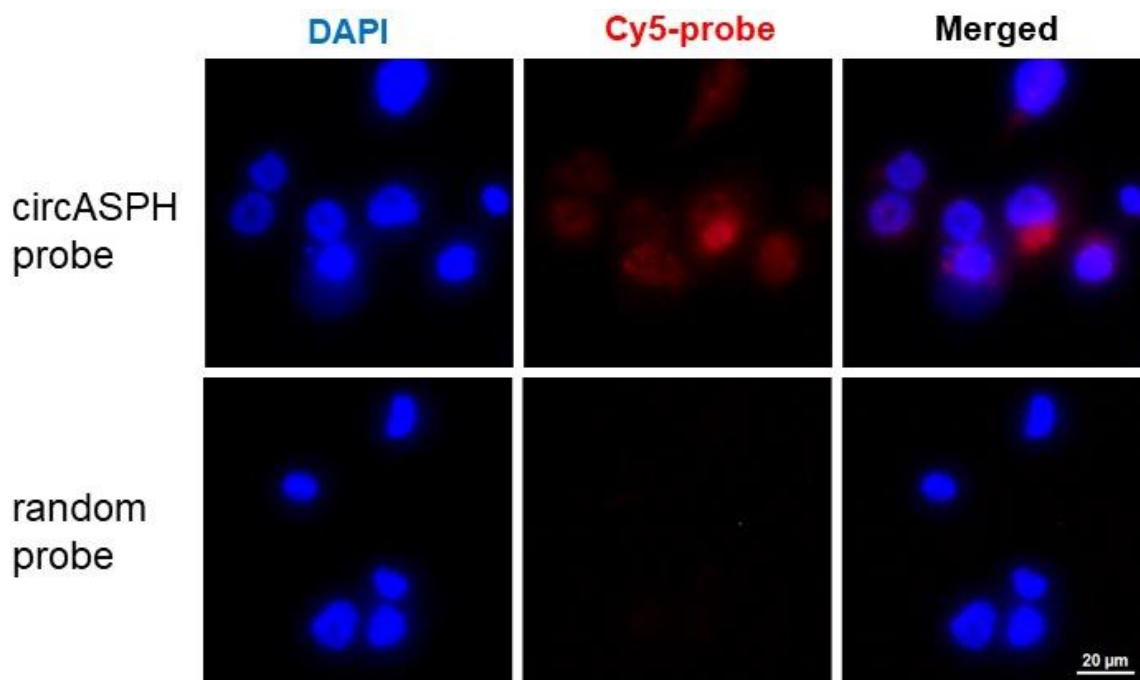


Figure 3.9 CircASP is primarily expressed in the cytosol of PMA-treated THP-1 cells by RNA-FISH with Cyanine 5-labelled probes. THP-1 cells were differentiated with 25 ng/mL PMA for 48 h and rested in PMA-free media for 24 h. Cells were fixed, permeabilized, and hybridized overnight with 500 nM Cy5-labelled circASP probes (top) or random probes (bottom). Cell nuclei were also stained with DAPI prior to fluorescent imaging.

To validate the upregulation of circASP during M1 and M2 polarization found in the previous section, and to confirm cellular distribution of circASP, RNA-FISH was repeated using PMA-differentiated THP-1 cells that were untreated (Fig. 3.10, top panel) or polarized with IFN- γ + LPS for 24 h (Fig. 3.10, middle panel) or IL-4 for 12 h (Fig. 3.10, bottom panel). Difference in signal intensity between the treatments confirmed circASP overexpression and cellular distribution during M1 or M2 polarization (Fig. 3.10).

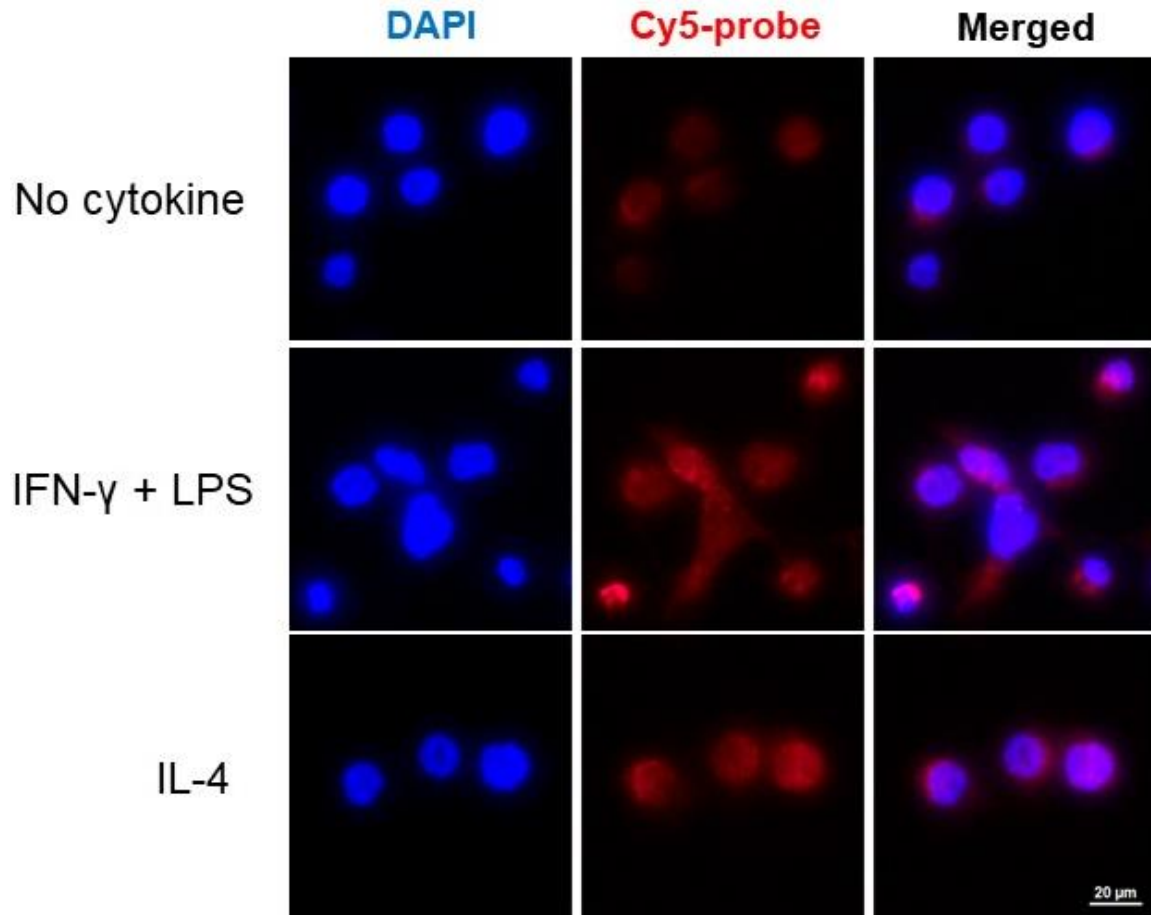


Figure 3.10 CircASPH upregulation in polarized THP-1 macrophages determined by RNA-FISH. THP-1 cells were differentiated with 25 ng/mL PMA for 48 h and rested in PMA-free media for 24 h, then treated with 20 ng/mL IFN- γ + 5 ng/mL LPS for 24 h or 30 ng/mL IL-4 for 12 h. Cells without cytokine stimulation were used as a control. Cells were fixed, permeabilized, and hybridized overnight with 500 nM Cy5-labelled circASPH probes. Cell nuclei were also stained with DAPI prior to fluorescent imaging. Images were merged using Image J. Top: control cells without cytokine stimulation; Middle: cells treated with IFN- γ + LPS; Bottom: cells treated with IL-4.

3.8 CircASPH siRNA knocks down circASPH expression

To validate the efficacy of the designed siRNA against the BSJ of circASPH (named as si-circASPH), PMA-differentiated THP-1 cells were transfected with si-circASPH or negative control (NC) siRNA for 1 d. Total RNA was collected, cDNA was synthesized, and the expression of circASPH-1 and circASPH-2 was quantified through qPCR. Si-circASPH achieved over 50% knockdown of circASPH expression in both isoforms (Fig. 3.11).

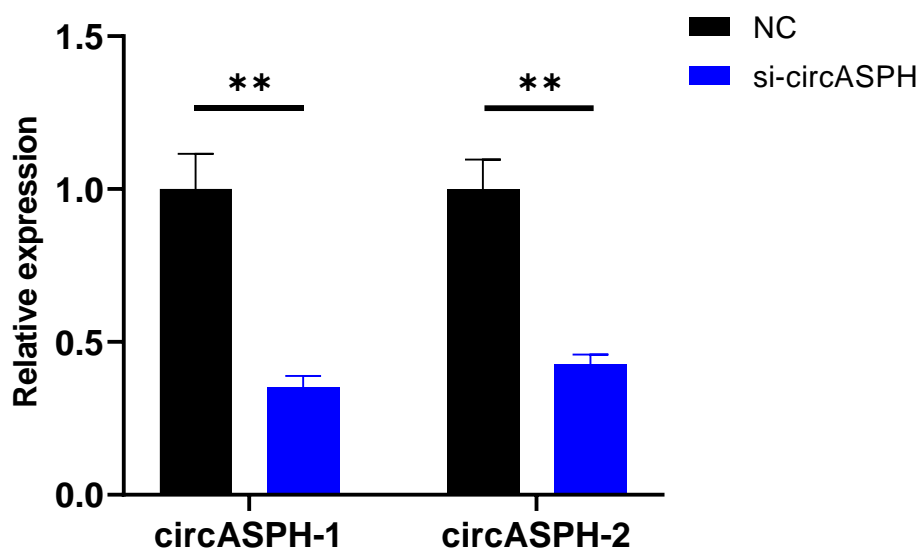


Figure 3.11 Transfection with anti-circASPH siRNA attenuates circASPH expression. THP-1 cells were differentiated with 25 ng/mL PMA for 48 h and rested in PMA-free media for 24 h, then transfected with control (NC) or anti-circASPH siRNA for 1 d. Total RNA was harvested and cDNA was synthesized. Relative expression of two isoforms of circASPH (circASPH-1 and circASPH-2) was quantified through qPCR using the $2^{-\Delta\Delta C_t}$ method, with 18S as an internal control, normalized to NC. Data represented as mean \pm SEM (n = 3). **, p < 0.01 by student's t-test.

3.9 CircASPH siRNA downregulates M1 genes and upregulates M2 genes

To investigate the effect of circASPH knockdown on M1 and M2 polarization gene markers, PMA-differentiated THP-1 cells were transfected with NC siRNA or si-circASPH 6 h before stimulation with IFN- γ + LPS or IL-4 for 1 d. Expression of M1 (IL-1 β , IL-6, TNF- α , CXCL9, and STAT1) or M2 (ALOX15 and CCL17) gene markers, circASPH isoforms, and linear ASPH were quantified through qRT-PCR. In M1 polarized macrophages, both circASPH isoforms and linear ASPH were knocked down (Fig. 3.12, top panel), and IL-1 β , TNF- α , CXCL9, and STAT1 were all downregulated, while IL-6 was unchanged (Fig. 3.12, bottom panel). In M2 polarized macrophages, neither circASPH isoform nor linear ASPH was reduced (Fig. 3.13, top panel), whereas ALOX15 and CCL17 were both upregulated (Fig. 3.13, bottom panel).

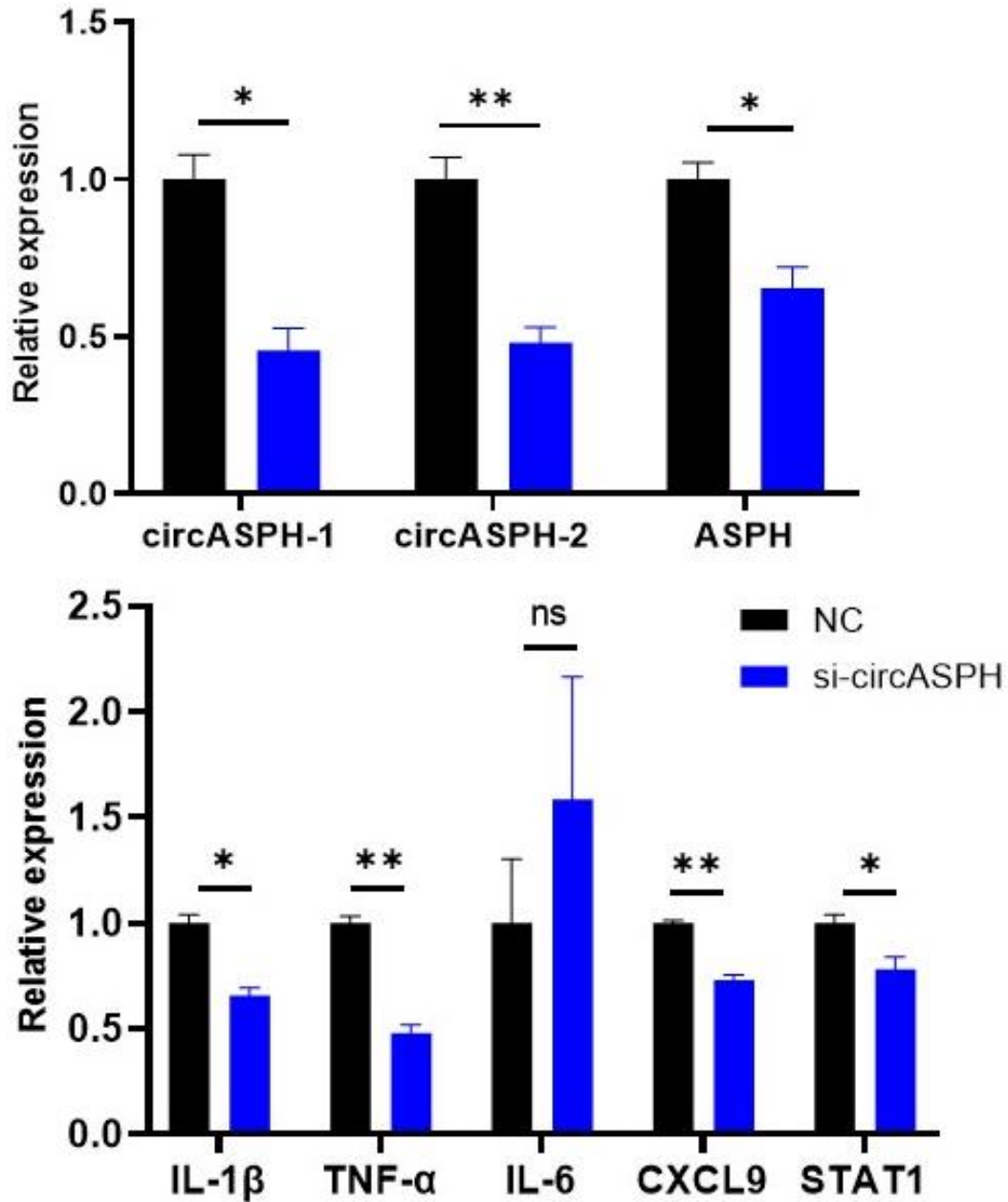


Figure 3.12 CircASPH knockdown attenuates the expression of IFN- γ + LPS-stimulated M1 gene markers. THP-1 cells were differentiated with 25 ng/mL PMA for 48 h and rested in PMA-free media for 24 h, then transfected with NC or anti-circASPH siRNA 6 h prior to stimulation with 20 ng/mL IFN- γ + 5 ng/mL LPS for 24 h. Total RNA was harvested and cDNA was synthesized. Relative expression of two isoforms of circASPH, linear ASPH, and M1 gene markers were quantified through qPCR using the $2^{-\Delta\Delta C_t}$ method, with 18S as an internal control. Data represented as mean \pm SEM (n = 3). *, p < 0.05; **, p < 0.01 by student's t-test.

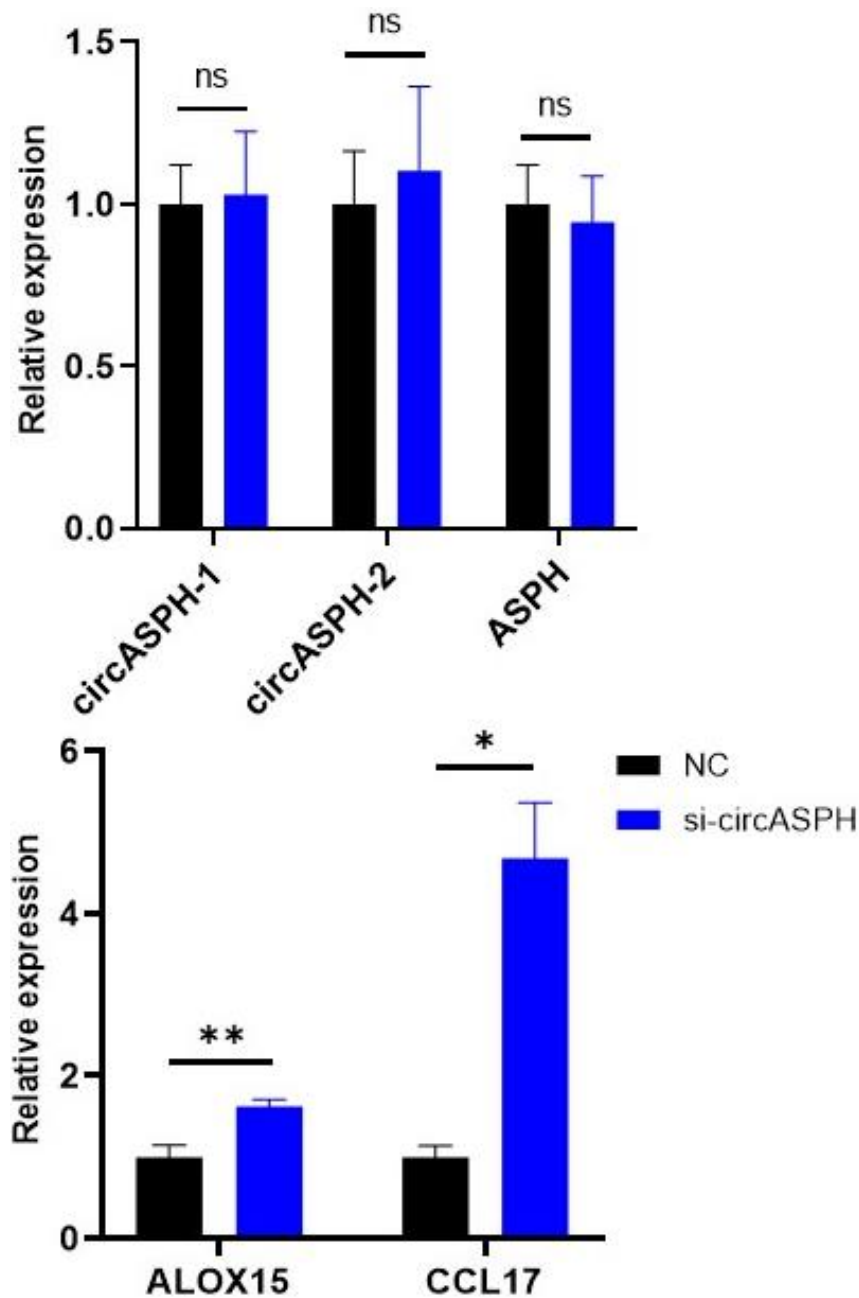


Figure 3.13 Pre-transfection with circASPH siRNA upregulates IL-4-stimulated M2 gene marker expressions. THP-1 cells were differentiated with 25 ng/mL PMA for 48 h and rested in PMA-free media for 24 h, then transfected with NC or anti-circASPH siRNA 6 h prior to stimulation with 30 ng/mL IL-4 for 24 h. Total RNA was harvested and cDNA was synthesized. Relative expression of two isoforms of circASPH, linear ASPH, and M2 gene markers were quantified through qPCR using the $2^{-\Delta\Delta C_t}$ method, with 18S as an internal control. Data represented as mean \pm SEM (n = 3). *, p < 0.05; **, p < 0.01 by student's t-test.

3.10 CircASPH knockdown attenuates cytokine secretion during M1 polarization

To validate the effect of circASPH knockdown on THP-1 macrophage cytokine secretion during M1 polarization, cell medium collected from PMA-differentiated THP-1 cells transfected with siRNA and treated with IFN- γ + LPS in the previous section were sent to be analyzed by a multiplex immunoassay including 15 cytokines (GM-CSF, IFN γ , IL-1 β , IL-1RA, IL-2, IL-4, IL-5, IL-6, IL-8, IL-10, IL-12p40, IL-12p70, IL-13, MCP-1, and TNF α). Knockdown of circASPH was associated with reduced secretion of IL-1Ra, IL-4, IL-6, IL-12p40, MCP-1, and TNF- α , while the remaining cytokines were not significantly changed (Fig. 3.14). These results further support the role of circASPH in promoting M1 polarization and function.

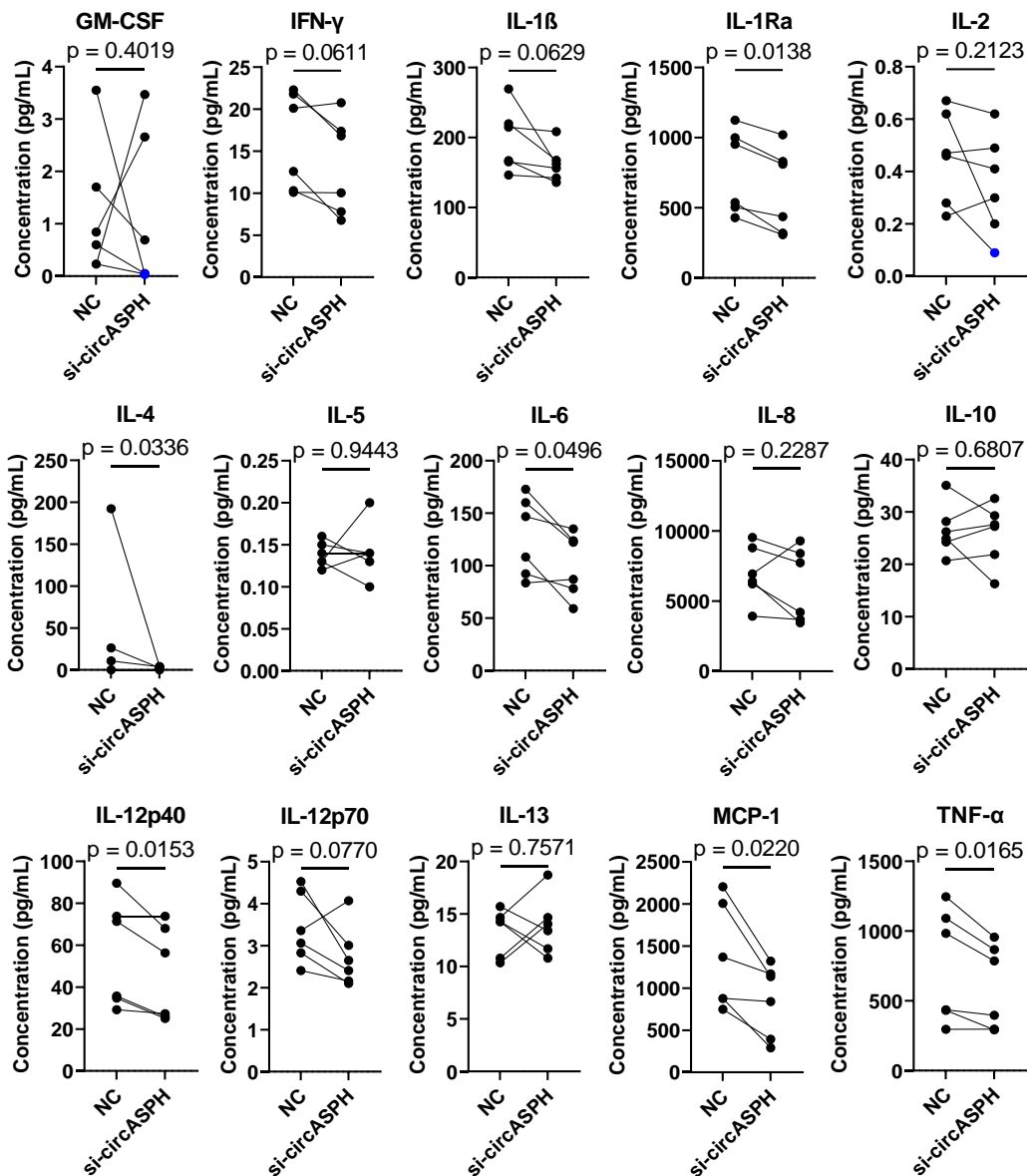


Figure 3.14 CircASP1 knockdown reduces cytokine production during M1

polarization. THP-1 cells were differentiated with 25 ng/mL PMA for 48 h and rested in PMA-free media for 24 h, then transfected with NC or anti-circASP1 siRNA 6 h prior to stimulation with 20 ng/mL IFN- γ + 5 ng/mL LPS for 24 h. Cell media was collected, and cytokine concentrations were quantified by multiplex cytokine immunoassay (n = 6).

Blue data points indicate values out of range below the standard curve, and were assigned the lowest standard value. P-values calculated from paired ratio t-test.

3.11 CircASPH knockdown reduces STAT1 protein expression

To investigate the signal pathway through which circASPH regulates macrophage polarization, western blotting was performed for total and phosphorylated NF- κ B p65 and STAT1, two key transcription factors for M1 gene expression, in THP-1 cells transfected with si-circASPH and polarized with IFN- γ + LPS. CircASPH knockdown was associated with downregulation of total STAT1 expression, while total NF- κ B expression and phosphorylation for both transcription factors were unchanged (Figure 3.15).

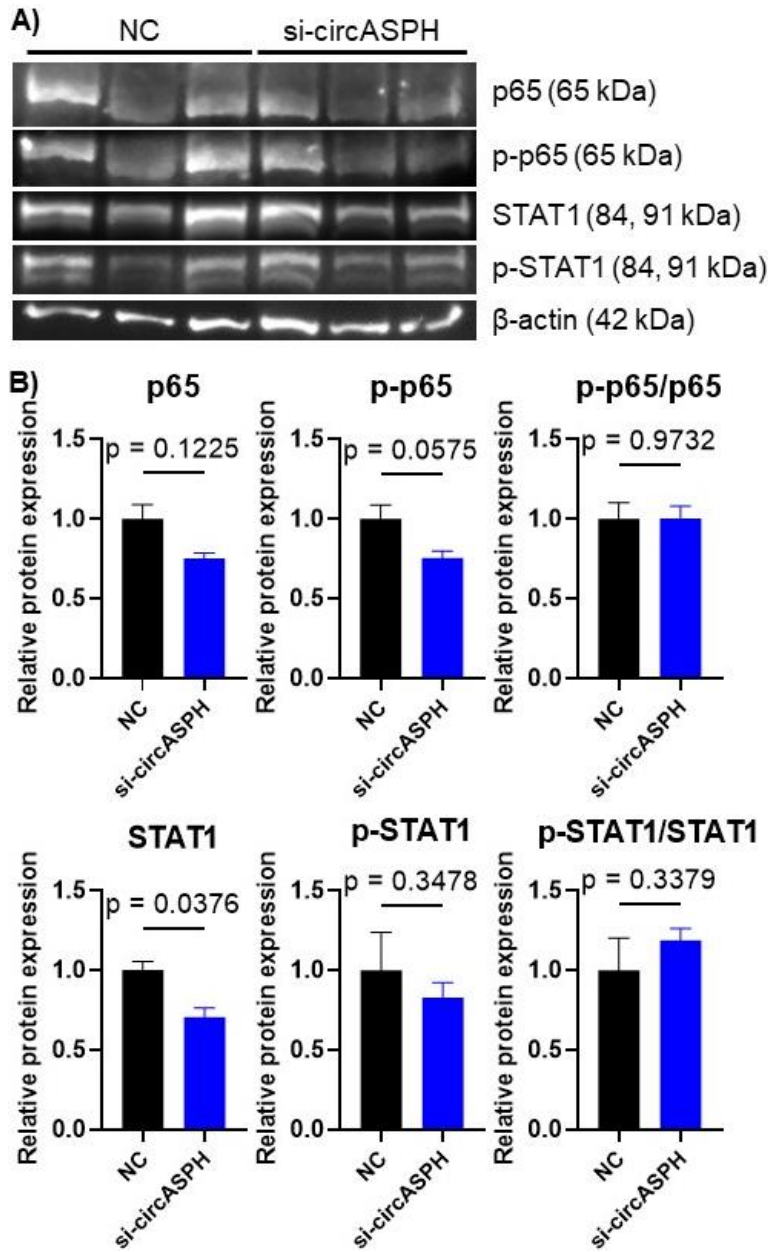


Figure 3.15 CircASPH knockdown reduces STAT1 protein during M1 polarization.

THP-1 cells were differentiated with 25 ng/mL PMA for 48 h and rested in PMA-free media for 24 h, then transfected with NC or anti-circASPH siRNA 6 h prior to stimulation with 20 ng/mL IFN- γ + 5 ng/mL LPS for 24 h. Cells were harvested and total protein was extracted using RIPA buffer. (A) Western blotting images of phosphorylated and total NF- κ B p65 and STAT1 (n = 3). (B) Relative expression of phosphorylated and total NF- κ B p65 and STAT1 proteins. Densitometry analysis of (A) was conducted using Image J and normalized using β -actin, represented as mean \pm SEM. P-values calculated from paired ratio t-test.

3.12 CircASPH knockdown does not increase cell death

To investigate the effect of circASPH knockdown on cell death, PMA-differentiated THP-1 cells were transfected with NC siRNA or si-circASPH, treated with PI which was used to detect dead cells, and dynamically imaged by a Cytation 5 connected to a BioTek BioSpa 8. Eight bright field and red fluorescence images per well were taken every 2 h, and IFN- γ + LPS was added right before the 4th read (6 h after transfection). The resulting cell death curve shows that IFN- γ + LPS stimulation caused significant cell death compared with control cells (Fig. 3.16). Cells transfected with the two siRNAs showed similar rates of cell death, indicating that the results in previous sections are unlikely to have been affected by cell death (Fig. 3.16).

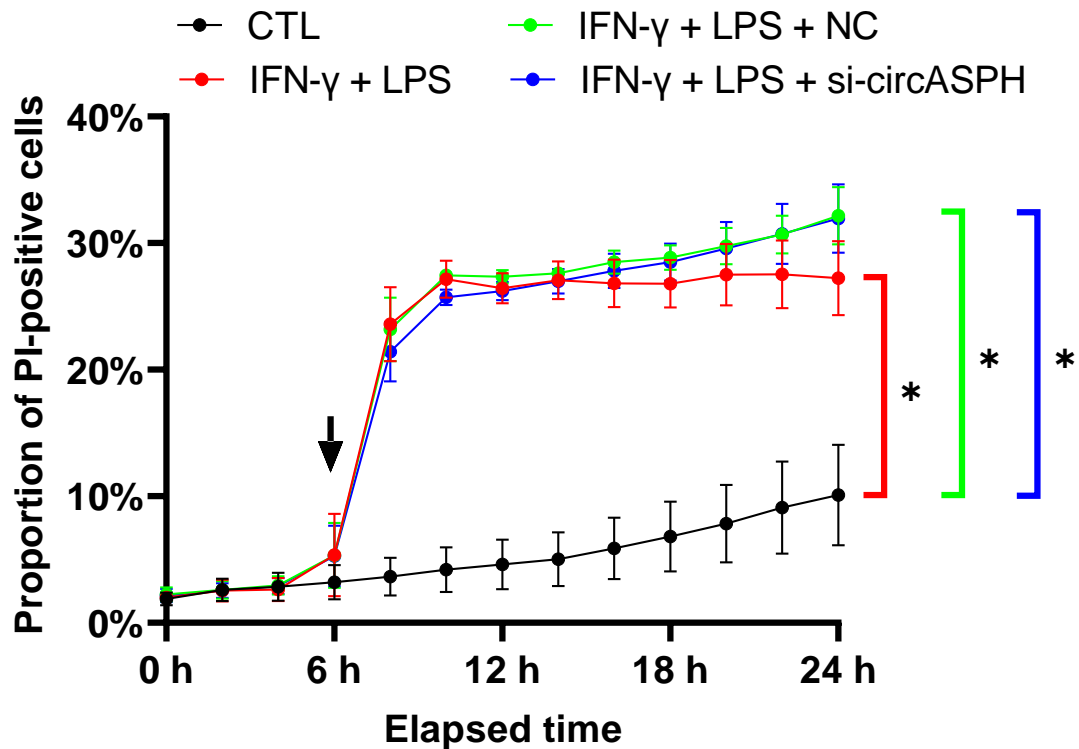


Figure 3.16 Cell death curve of PMA-treated THP-1 cells after circASPH

knockdown and IFN- γ + LPS treatment. THP-1 cells were differentiated with 25 ng/mL PMA for 48 h and rested in PMA-free media for 24 h, then transfected with NC or anti-circASPH siRNA with added 1 μ g/mL propidium iodide. Cells were dynamically imaged by a Cytation 5 every 2 h at 8 locations per well. The time where 20 ng/mL IFN- γ and 5 ng/mL LPS were added is indicated by the black arrow. Data presented as mean \pm SEM of proportions of PI-positive cells summed across all locations per well at each time point (n = 3). Lines indicating statistical tests were coloured to match one of the groups in the test conducted to avoid ambiguity. *, p < 0.05 by one-way ANOVA.

Chapter 4

4 Discussion and Conclusion

In this work, I confirmed the overexpression of circASPH-1 and circASPH-2 in septic PBMCs at ICU-AD compared to ICU-DC, and showed that circASPH levels of both isoforms are correlated with IL-12p70 at ICU-AD and with IL-5 at ICU-DC. Using a THP-1 model of macrophage polarization, I demonstrated that circASPH promotes M1 polarization and cytokine secretion, potentially through upregulating the M1 transcription factor STAT1.

4.1 CircASPH upregulated in septic PBMCs at ICU-AD and associated with IL-12 and IL-5 secretion

We have previously identified circASPH to be upregulated at ICU-AD in septic PBMCs through RNAseq. In this work, I validated the upregulation of two circASPH isoforms through qPCR in a larger sample size of sepsis patients, again comparing ICU-AD with ICU-DC. From the multiplex cytokine assay results, I also reported the overexpression of GM-CSF, IL-1Ra, IL-2, IL-6, and IL-10 in sepsis patients at ICU-AD compared with ICU-DC. My results are similar to a previous study by Wu and colleagues, who also reported a significant decrease in plasma IL-6 and IL-10 levels in severe sepsis patients 6 days post-ICU-AD compared with ICU-AD, but no change in plasma IL-1 β , IL12, or TNF- α levels ⁸⁶.

I also found that circASPH expression positively correlates with IL-12p70 levels at ICU-AD and IL-5 levels at ICU-DC. Since IL-12 is a pro-inflammatory Th1 cytokine while IL-5 is a Th2 cytokine, these results indicate that circASPH is involved with both Th1

responses in the early stage of sepsis and Th2 responses in the later stage. Though IL-12p70 was not shown to be significantly changed between ICU-AD and ICU-DC in the current cohort, Wu and colleagues found that plasma IL-12 levels are reduced in sepsis patients at ICU-AD compared to healthy controls, and further reduced 6 days post-ICU-AD in survivors of severe sepsis⁸⁶. IL-12 is produced by monocytes, macrophages, and dendritic cells after TLR4 stimulation, and it activates natural killer cells as well as induce the differentiation of Th1 effector cells⁸⁷. IL-12 production is shown to be protective against sepsis mortality. Weighardt and colleagues found that defective monocyte IL-12 production was an independent predictive factor for sepsis mortality⁸⁸, and Wu and colleagues reported a significantly increased IL-12 response in PBMCs from sepsis survivors 6 days post-ICU-AD compared with ICU-AD, while no change was observed in non-survivors⁸⁶. IL-5 is a Th2 cytokine that is thought to participate mainly in eosinophil maturation, and IL-5 knockout was shown to promote M1 macrophage polarization and exacerbate sepsis-induced cardiac injury in mice⁸⁹. Lynch and colleagues showed that expression for the IL-5 receptor was induced in neutrophils and monocytes during the acute phase of sepsis and decreased after resolution of inflammation, indicating the importance of IL-5 signaling in these cells during sepsis⁹⁰. They also showed that high IL-5 levels were associated with improved patient outcomes in sepsis, and proposed that IL-5 improves neutrophil and monocyte recruitment, as well as macrophage functions and survival⁹⁰. Taken together, my results indicate the potential of circASPH as a positive regulator of IL-12 and IL-5 production, and thus circASPH levels may be associated with patient outcomes. Validation of these results in a larger

cohort, along with increased understanding of the mechanism behind this association, may inspire novel targets to improve sepsis outcome.

4.2 CircASPH expression in THP-1 model of macrophage polarization

Much of the initial immune response in sepsis is driven by myeloid cells, and macrophages are first responders to infection, engulfing invading pathogens and secreting a wide array of cytokines to recruit and differentiate other immune cells²⁸. Most biomarkers of sepsis are produced primarily by monocyte or macrophage³, suggesting that a regulator on macrophage phenotype and function would have cascading effects on the systemic immune response in sepsis. In this study, I investigated the role of circASPH in a THP-1 model of macrophage polarization because THP-1 is one of the most popular cell lines used in the study of macrophages. THP-1 is a monocytic leukemia cell line that can be differentiated into macrophage-like cells through PMA stimulation. Previous studies have characterized the upregulation of M1 genes due to PMA stimulation, and recommended using lower concentrations of PMA³⁹, along with a period of rest in PMA-free medium³⁸, to improve M2 polarization. I characterized the phenotypic changes in THP-1 cells exposed to 25 ng/mL PMA before replacing with PMA-free medium, using IL-1 β , one of the most sensitive M1 genes, as a marker for M1 phenotype. I found that 48 h of PMA stimulation resulted in a 19-fold increase of IL-1 β , which was returned to its baseline level after 24 h of rest in PMA-free medium. Thus, I used this protocol for my *in vitro* model to ensure effectiveness in both M1 and M2 polarization. I also found that circASPH-1 was downregulated and circASPH-2 upregulated 48 h after PMA differentiation, indicating a difference between basal circASPH expression between THP-

1 monocytes and macrophages, thus supporting the involvement of circASPH in THP-1 phenotypic changes.

For the stimulants for polarization, Baxter *et al.* recommended 20 ng/mL IFN- γ + 250 ng/mL LPS for M1 polarization and 30 ng/mL IL-4 for M2 polarization, which formed the basis of my model ³⁸. However, another study cautioned against using high LPS doses with IFN- γ , reporting 25% cell death after 24 h stimulation with 20 ng/mL IFN- γ and only 1 ng/mL LPS ⁹¹. This was later confirmed by my cell death assay results showing the same toxicity after 4 h stimulation with 20 ng/mL IFN- γ and 5 ng/mL LPS. Overall, I chose 5 ng/mL LPS to achieve substantial M1 response in the absence of other immune cells while avoiding excessive cell death caused by high LPS concentrations. My model of THP-1 macrophage polarization was validated by quantifying transcription of gene markers used by Baxter *et al.*: IL-1 β , TNF- α , IL-6, CXCL9, and STAT1 for M1, and ALOX15 and CCL17 for M2 ³⁸. I found that transcription of M1 cytokines peaked at 6 h, while all gene markers were upregulated by 1 d. Because the early phase of sepsis can last several days, I chose 1 d as the earliest time point to ensure validity of my model and to maintain consistency between M1 and M2 polarization protocols.

I showed that circASPH levels changed dynamically in polarized macrophages, and that both isoforms of circASPH are upregulated in M1 macrophages after 1 d of stimulation and in M2 macrophages after 12 h of stimulation. I found circASPH to be primarily localized in the cytoplasm by RNA-FISH, which is consistent with most exonic circRNAs ⁴⁴. Because both isoforms of circASPH have the same BSJ sequences and the probe sequence selected is complementary to the BSJ, our RNA-FISH detected both

isoforms of circASPH-1 and circASPH-2, which differs from qRT-PCR that specifically measures each isoform with specific primers.

I further compared the circASPH and ASPH expression profile during THP-1 macrophage polarization. I found a substantial downregulation of the linear ASPH compared to circASPH during the first 12 h of M1 polarization, while linear ASPH was upregulated compared to circASPH throughout the majority of M2 polarization. The significance of the circular-to-linear RNA ratio is that it quantifies the splicing preference of ASPH pre-mRNA, with my data suggesting that backsplicing is favoured during M1 polarization while conventional splicing is favoured during M2. Detailed investigation into the mechanism behind this phenomenon would not only shed light on the biogenesis of circASPH, but also on the possible downstream effects of circASPH/ASPH expression changes on macrophage polarization.

4.3 CircASPH knockdown reduces M1 cytokine production and STAT1 expression

I investigated the role of circASPH in M1 polarization through loss-of-function experiments with an siRNA designed to target the BSJ of circASPH. CircASPH knockdown reduced transcription of cytokines IL-1 β , TNF- α , and CXCL9, and reduced IL-1Ra, IL-4, IL-6, IL-12p40, MCP-1, and TNF- α secretion. CircASPH siRNA also reduced STAT1 at the mRNA and protein levels. These data suggest that circASPH promotes M1 polarization. However, there is no difference in phosphorylated STAT1 and total and phosphorylated NF- κ B at the time point investigated. This could be due to 24 h being too late in the macrophage polarization process, and the cell has compensated for

the effects of circASPH knockdown. Future studies should investigate earlier time points to better assess the effect of circASPH knockdown on these targets.

STAT1 is a master regulator of M1 polarization effectors, and when phosphorylated by IFN- γ -induced JAK activation, dimerizes and translocates to the nucleus to activate a multitude of genes through their IFN- γ activation sequence²⁶. STAT1 activation enhances the effectiveness of the TLR/NF- κ B pathway by inhibiting IL-10 and STAT3, which are induced by NF- κ B to inhibit TLR signalling in a negative feedback loop⁹². IFN- γ also activates, through STAT1, the upregulation of proinflammatory cytokines TNF- α ⁹², IL-1⁹², IL-6⁹³, IL-12⁹⁴, and MCP-1⁹⁵, which my results showed either reduced transcription or translation after circASPH knockdown. Thus, I propose that circASPH promotes M1 polarization and cytokine release, possibly by upregulating the transcription factor STAT1. These cytokines are also of great clinical relevance. Bozza and colleagues reported elevated IL-1 β , IL-6, IL-7, IL-8, IL-10, IL-13, MCP-1, and TNF- α levels in septic shock patients compared to sepsis⁹⁶, while Mera and colleagues found MCP-1 levels to be positively correlated with Sepsis-related Organ Failure Assessment scores at ICU-AD, as well as elevated levels of IL-1 β , IL-6, IL-8, IL-12, IFN- γ , and TNF- α in non-survivors compared to survivors⁹⁷. These reports, along with my current results, support the putative effect of circASPH levels on sepsis severity and outcomes, and further investigations into the exact mechanism by which circASPH modulates macrophage cytokine production may aid development of novel immunomodulatory therapies in sepsis.

4.4 Pretreatment with circASPH siRNA and M2 polarization

The role of circASPH in M2 polarization is unclear. STAT1 competes with the M2 transcription factor STAT6 for binding to coactivator CREB-binding protein and to IFN- γ activation sequences to exert its effect ²⁶. In this study, I showed downregulation of STAT1 in THP-1 cells after circASPH knockdown, thus it is expected that circASPH knock down would promote M2 polarization. My results show that cells transfected with circASPH siRNA upregulated M2 gene markers ALOX15 and CCL17 after 24 h of IL-4 stimulation, but fail to show knockdown of circASPH at that time point. As our results for circASPH expression profile during M2 polarization show that circASPH levels decrease 24 h after IL-4 treatment and the decrease continued afterwards, it is possible that IL-4-induced reduction of circASPH dampens the effects of siRNA knockdown, leading to no significant difference in circASPH level between the cells pre-transfected with circASPH siRNA and NC siRNA. Nonetheless, I cannot directly link circASPH level to M2 polarization effectiveness. Future investigations with more time points and alternative M2 markers, or transfection with circASPH overexpression plasmids are required to confirm the involvement of circASPH in M2 polarization.

4.5 ASPH

As previously discussed, ASPH expression, as well as its relative abundance compared to circASPH, were significantly altered during macrophage polarization, indicating ASPH may participate in sepsis and macrophage polarization. In the circASPH loss-of-function experiments, ASPH is also consistently knocked down along with circASPH. The designed siRNA si-circASPH does bind to linear ASPH at the first 9 nt of its 5' end (Fig. S3). Thus, there is a small possibility that the reduction of ASPH mRNA is an off-target

effect of si-circASPH. However, it has been shown that circRNAs can affect the expression of their home gene through competition between canonical and backsplicing⁹⁸, and they can compete for RBP binding to regulate translation of their home gene^{69,99}. Thus, it is more likely that circASPH and ASPH regulate one another to modulate macrophage polarization, which needs to be further investigated. It can be hypothesized that increased ASPH expression enhances phagocytosis in macrophages through the increased production of junctate⁸⁴, though the exact mechanism by which ASPH enhances other M1 functions has never been investigated. Recently, Wang and colleagues described the putative function of circRNA transmembrane 7 superfamily member 3 in the upregulation of ASPH in THP-1 cells through sequestration of miR-206, which targets ASPH mRNA¹⁰⁰. They showed that upregulation of ASPH led to increased pro-inflammatory activities in THP-1 macrophages activated by low-density lipoprotein as a model of atherosclerosis¹⁰⁰. This work, along with my current findings, support the potential of circRNAs and ASPH in modulating M1 macrophage functions, and highlight the importance of further research into the role of ASPH in macrophages.

4.6 CircASPH and cell death

In the context of infection, macrophages may undergo inflammatory forms of cell death, such as pyroptosis and necroptosis, to recruit other immune cells and limit microbial replication, but uncontrolled macrophage death can lead to tissue damage and pathogen persistence¹⁰¹. Several circRNAs were shown to regulate cell death, including circANRIL⁵⁴ and circFoxo3¹⁰², and in this work, I investigated the relationship between circASPH expression and THP-1 macrophage cell death during M1 polarization. Using live cell imaging, I found that 20 ng/mL IFN- γ and 5 ng/mL LPS stimulation caused

more than 25% cell death within the first 4 hours, and that transfection with control siRNA did not cause significant cell death during M1 polarization. I also found that transfection with si-circASPH did not result in greater cell death compared with control siRNA, suggesting that circASPH is unlikely to participate in macrophage cell death pathways.

4.7 Limitations

Several limitations affect the generalizability and applicability of my results. The sample size in the clinical portion of the work is small, especially for a disease as complex and heterogeneous as sepsis. As such, the findings must be validated in a larger sample size. I also did not separate bulk PBMC by cell type, which is required to demonstrate circASPH overexpression in monocytes *in vivo*. For my *in vitro* results, much remains unknown regarding the specific time points when circASPH and ASPH expressions change, and whether that correspond with changes in macrophage effector genes. I also did not test the full range of M1 and M2 markers and effector genes, nor did I perform functional assays such as phagocytosis or migration assays. There are also phenotypic differences between THP-1 cell line and macrophages *in vivo*, with multiple studies reporting a limited capability for THP-1 macrophages to polarize towards M2^{37,103}. As such, my findings should be confirmed in bone-marrow derived macrophages and an animal model of sepsis to validate the biological relevance of circASPH. Finally, I did not investigate the specific mechanism by which circASPH regulates ASPH levels or vice versa, nor did I investigate the specific miRNA or protein interaction that leads to the regulation of STAT1 and cytokines. Future investigations into both questions would

provide a clearer understanding of circASPH and ASPH in macrophage function and allow assessment of their potential as therapeutic targets.

4.8 Concluding Remarks and Future Directions

In conclusion, my work revealed a novel potential regulator of macrophage polarization and function. I showed that circASPH was overexpressed in septic PBMCs at ICU-AD compared to ICU-DC, while its expression fluctuates in polarized THP-1 macrophages. Through *in vitro* experiments, I showed that circASPH knockdown overall attenuated M1 polarization and encouraged M2 polarization; however, my profiling of circASPH and ASPH expression during cytokine stimulation of macrophages suggests a complex interaction between the linear and circular isoforms that together modulate macrophage polarization. I showed that circASPH knock down reduced production for several major macrophage cytokines, which potentially links circASPH to the cytokine storm and systemic immune dysregulation seen in sepsis. Finally, I also showed evidence of circASPH possibly exerting its effects through the STAT1 pathway through upregulation of STAT1 protein expression.

Future investigations are required to confirm the upregulation of circASPH in septic monocytes and macrophages, to elucidate the specific mechanism through which circASPH modulates macrophage function, and to evaluate the clinical potential of circASPH using animal models of sepsis.

Chapter 5

5 References

1. Singer, M. *et al.* The Third International Consensus Definitions for Sepsis and Septic Shock (Sepsis-3). *JAMA* **315**, 801 (2016).
2. Rudd, K. E. *et al.* Global, regional, and national sepsis incidence and mortality, 1990–2017: analysis for the Global Burden of Disease Study. *Lancet* **395**, 200–211 (2020).
3. Huang, M., Cai, S. & Su, J. The Pathogenesis of Sepsis and Potential Therapeutic Targets. *Int. J. Mol. Sci.* **20**, 5376 (2019).
4. Hotchkiss, R. S., Monneret, G. & Payen, D. Sepsis-induced immunosuppression: from cellular dysfunctions to immunotherapy. *Nat. Rev. Immunol.* **13**, 862–874 (2013).
5. Nedeva, C., Menassa, J. & Puthalakath, H. Sepsis: Inflammation Is a Necessary Evil. *Front. Cell Dev. Biol.* **7**, (2019).
6. Hotchkiss, R. S., Monneret, G. & Payen, D. Immunosuppression in sepsis: a novel understanding of the disorder and a new therapeutic approach. *Lancet Infect. Dis.* **13**, 260–268 (2013).
7. Nedeva, C. Inflammation and Cell Death of the Innate and Adaptive Immune System during Sepsis. *Biomolecules* **11**, 1011 (2021).
8. Rhodes, A. *et al.* Surviving Sepsis Campaign. *Crit. Care Med.* **45**, 486–552 (2017).
9. Seigel, T. A. *et al.* Inadequacy of Temperature and White Blood Cell Count in Predicting Bacteremia in Patients with Suspected Infection. *J. Emerg. Med.* **42**, 254–259 (2012).

10. Hoser, G. A., Skirecki, T., Złotorowicz, M., Zielińska-Borkowska, U. & Kawiak, J. Absolute counts of peripheral blood leukocyte subpopulations in intraabdominal sepsis and pneumonia-derived sepsis: a pilot study. *Folia Histochem. Cytobiol.* **50**, 420–426 (2012).
11. Xiao, W. *et al.* A genomic storm in critically injured humans. *J. Exp. Med.* **208**, 2581–2590 (2011).
12. Davenport, E. E. *et al.* Genomic landscape of the individual host response and outcomes in sepsis: a prospective cohort study. *Lancet Respir. Med.* **4**, 259–271 (2016).
13. Sweeney, T. E. *et al.* Unsupervised Analysis of Transcriptomics in Bacterial Sepsis Across Multiple Datasets Reveals Three Robust Clusters. *Crit. Care Med.* **46**, 915–925 (2018).
14. Leligdowicz, A. *et al.* Functional Transcriptomic Studies of Immune Responses and Endotoxin Tolerance in Early Human Sepsis. *Shock* **57**, 180–190 (2022).
15. Wang, F. *et al.* Integrating bulk and single-cell sequencing reveals the phenotype-associated cell subpopulations in sepsis-induced acute lung injury. *Front. Immunol.* **13**, (2022).
16. Wang, T. *et al.* Single-cell RNA sequencing reveals the sustained immune cell dysfunction in the pathogenesis of sepsis secondary to bacterial pneumonia. *Genomics* **113**, 1219–1233 (2021).
17. Chaintreuil, P. *et al.* The generation, activation, and polarization of monocyte-derived macrophages in human malignancies. *Front. Immunol.* **14**, (2023).
18. Sreejit, G., Fleetwood, A. J., Murphy, A. J. & Nagareddy, P. R. Origins and diversity of macrophages in health and disease. *Clin. Transl. Immunol.* **9**, (2020).
19. Shapouri-Moghaddam, A. *et al.* Macrophage plasticity, polarization, and function in health and disease. *J. Cell. Physiol.* **233**, 6425–6440 (2018).

20. Stein, M., Keshav, S., Harris, N. & Gordon, S. Interleukin 4 potently enhances murine macrophage mannose receptor activity: a marker of alternative immunologic macrophage activation. *J. Exp. Med.* **176**, 287–292 (1992).
21. Mills, C. D., Kincaid, K., Alt, J. M., Heilman, M. J. & Hill, A. M. M-1/M-2 Macrophages and the Th1/Th2 Paradigm. *J. Immunol.* **164**, 6166–6173 (2000).
22. Kumar, V. Targeting macrophage immunometabolism: Dawn in the darkness of sepsis. *Int. Immunopharmacol.* **58**, 173–185 (2018).
23. Murray, P. J. *et al.* Macrophage Activation and Polarization: Nomenclature and Experimental Guidelines. *Immunity* **41**, 14–20 (2014).
24. Ciesielska, A., Matyjek, M. & Kwiatkowska, K. TLR4 and CD14 trafficking and its influence on LPS-induced pro-inflammatory signaling. *Cell. Mol. Life Sci.* **78**, 1233–1261 (2021).
25. Christian, F., Smith, E. & Carmody, R. The Regulation of NF- κ B Subunits by Phosphorylation. *Cells* **5**, 12 (2016).
26. Ohmori, Y. & Hamilton, T. A. STAT6 Is Required for the Anti-inflammatory Activity of Interleukin-4 in Mouse Peritoneal Macrophages. *J. Biol. Chem.* **273**, 29202–29209 (1998).
27. Levy, D. E. & Darnell, J. E. STATs: transcriptional control and biological impact. *Nat. Rev. Mol. Cell Biol.* **3**, 651–662 (2002).
28. Romero, C. R. *et al.* The role of interferon- γ in the pathogenesis of acute intra-abdominal sepsis. *J. Leukoc. Biol.* **88**, 725–735 (2010).
29. Venet, F., Demaret, J., Gossez, M. & Monneret, G. Myeloid cells in sepsis-acquired immunodeficiency. *Ann. N. Y. Acad. Sci.* **1499**, 3–17 (2021).
30. Pena, O. M., Pistolic, J., Raj, D., Fjell, C. D. & Hancock, R. E. W. Endotoxin Tolerance Represents a Distinctive State of Alternative Polarization (M2) in

- Human Mononuclear Cells. *J. Immunol.* **186**, 7243–7254 (2011).
31. Takeyama, N., Tanaka, T., Yabuki, T., Nakatani, K. & Nakatani, T. Effect of interferon gamma on sepsis-related death in patients with immunoparalysis. *Crit. Care* **8**, P207 (2004).
 32. Cheng, S.-C. *et al.* Broad defects in the energy metabolism of leukocytes underlie immunoparalysis in sepsis. *Nat. Immunol.* **17**, 406–413 (2016).
 33. Mathias, B., Szpila, B. E., Moore, F. A., Efron, P. A. & Moldawer, L. L. A Review of GM-CSF Therapy in Sepsis. *Medicine (Baltimore)*. **94**, e2044 (2015).
 34. Tsuchiya, S. *et al.* Establishment and characterization of a human acute monocytic leukemia cell line (THP-1). *Int. J. Cancer* **26**, 171–176 (1980).
 35. Auwerx, J. The human leukemia cell line, THP-1: A multifaceted model for the study of monocyte-macrophage differentiation. *Experientia* **47**, 22–31 (1991).
 36. Kim, Y. K., Hwang, J. H. & Lee, H. T. Differential susceptibility to lipopolysaccharide affects the activation of toll-like-receptor 4 signaling in THP-1 cells and PMA-differentiated THP-1 cells. *Innate Immun.* **28**, 122–129 (2022).
 37. Nascimento, C. R., Rodrigues Fernandes, N. A., Gonzalez Maldonado, L. A. & Rossa Junior, C. Comparison of monocytic cell lines U937 and THP-1 as macrophage models for in vitro studies. *Biochem. Biophys. Reports* **32**, 101383 (2022).
 38. Baxter, E. W. *et al.* Standardized protocols for differentiation of THP-1 cells to macrophages with distinct M(IFN γ +LPS), M(IL-4) and M(IL-10) phenotypes. *J. Immunol. Methods* **478**, 112721 (2020).
 39. Maeß, M. B., Wittig, B., Cignarella, A. & Lorkowski, S. Reduced PMA enhances the responsiveness of transfected THP-1 macrophages to polarizing stimuli. *J. Immunol. Methods* **402**, 76–81 (2014).

40. Guo, W., Wang, Z., Wang, S., Liao, X. & Qin, T. Transcriptome sequencing reveals differential expression of circRNAs in sepsis induced acute respiratory distress syndrome. *Life Sci.* **278**, 119566 (2021).
41. HSU, M.-T. & COCA-PRADOS, M. Electron microscopic evidence for the circular form of RNA in the cytoplasm of eukaryotic cells. *Nature* **280**, 339–340 (1979).
42. Greene, J. *et al.* Circular RNAs: Biogenesis, Function and Role in Human Diseases. *Front. Mol. Biosci.* **4**, (2017).
43. Chen, L.-L. The biogenesis and emerging roles of circular RNAs. *Nat. Rev. Mol. Cell Biol.* **17**, 205–211 (2016).
44. Kristensen, L. S. *et al.* The biogenesis, biology and characterization of circular RNAs. *Nat. Rev. Genet.* **20**, 675–691 (2019).
45. Chen, L.-L. & Yang, L. Regulation of circRNA biogenesis. *RNA Biol.* **12**, 381–388 (2015).
46. Li, X. *et al.* A unified mechanism for intron and exon definition and back-splicing. *Nature* **573**, 375–380 (2019).
47. Altesha, M., Ni, T., Khan, A., Liu, K. & Zheng, X. Circular RNA in cardiovascular disease. *J. Cell. Physiol.* **234**, 5588–5600 (2019).
48. Ouyang, Q. *et al.* Using plasma circRNA_002453 as a novel biomarker in the diagnosis of lupus nephritis. *Mol. Immunol.* **101**, 531–538 (2018).
49. Li, Y. *et al.* Circular RNA is enriched and stable in exosomes: a promising biomarker for cancer diagnosis. *Cell Res.* **25**, 981–984 (2015).
50. Jeck, W. R. *et al.* Circular RNAs are abundant, conserved, and associated with ALU repeats. *RNA* **19**, 141–157 (2013).
51. Hansen, T. B. *et al.* Natural RNA circles function as efficient microRNA sponges.

- Nature* **495**, 384–388 (2013).
52. Memczak, S. *et al.* Circular RNAs are a large class of animal RNAs with regulatory potency. *Nature* **495**, 333–338 (2013).
 53. Guo, J. U., Agarwal, V., Guo, H. & Bartel, D. P. Expanded identification and characterization of mammalian circular RNAs. *Genome Biol.* **15**, 409 (2014).
 54. Holdt, L. M. *et al.* Circular non-coding RNA ANRIL modulates ribosomal RNA maturation and atherosclerosis in humans. *Nat. Commun.* **7**, 12429 (2016).
 55. Fang, Y. *et al.* Screening of circular RNAs and validation of circANKRD36 associated with inflammation in patients with type 2 diabetes mellitus. *Int. J. Mol. Med.* (2018) doi:10.3892/ijmm.2018.3783.
 56. Hanan, M., Soreq, H. & Kadener, S. CircRNAs in the brain. *RNA Biol.* **14**, 1028–1034 (2017).
 57. Hsiao, K.-Y. *et al.* Noncoding Effects of Circular RNA CCDC66 Promote Colon Cancer Growth and Metastasis. *Cancer Res.* **77**, 2339–2350 (2017).
 58. Beltrán-García, J., Osca-Verdegal, R., Nacher-Sendra, E., Pallardó, F. V. & García-Giménez, J. L. Circular RNAs in Sepsis: Biogenesis, Function, and Clinical Significance. *Cells* **9**, 1544 (2020).
 59. Nie, M., Han, Y., Shen, Z. & Xie, H. Identification of circRNA and mRNA expression profiles and functional networks of vascular tissue in lipopolysaccharide-induced sepsis. *J. Cell. Mol. Med.* **24**, 7915–7927 (2020).
 60. Bao, X. *et al.* Characteristics of circular RNA expression of pulmonary macrophages in mice with sepsis-induced acute lung injury. *J. Cell. Mol. Med.* **23**, 7111–7115 (2019).
 61. Khan, H. N. *et al.* The circular RNA landscape in specific peripheral blood mononuclear cells of critically ill patients with sepsis. *Crit. Care* **24**, 423 (2020).

62. Tian, C. *et al.* Exosomal hsa_circRNA_104484 and hsa_circRNA_104670 may serve as potential novel biomarkers and therapeutic targets for sepsis. *Sci. Rep.* **11**, 14141 (2021).
63. Zhao, D. *et al.* CircN4bp1 Facilitates Sepsis-Induced Acute Respiratory Distress Syndrome through Mediating Macrophage Polarization via the miR-138-5p/EZH2 Axis. *Mediators Inflamm.* **2021**, 1–14 (2021).
64. Zhang, Y., Zhang, Y., Li, X., Zhang, M. & Lv, K. Microarray analysis of circular RNA expression patterns in polarized macrophages. *Int. J. Mol. Med.* **39**, 373–379 (2017).
65. Ng, W. L. *et al.* Inducible RasGEF1B circular RNA is a positive regulator of ICAM-1 in the TLR4/LPS pathway. *RNA Biol.* **13**, 861–871 (2016).
66. Deng, T. *et al.* Calcitonin gene-related peptide induces IL-6 expression in RAW264.7 macrophages mediated by mmu_circRNA_007893. *Mol. Med. Rep.* **16**, 9367–9374 (2017).
67. Huang, Z. *et al.* Identification of differentially expressed circular RNAs in human monocyte derived macrophages response to Mycobacterium tuberculosis infection. *Sci. Rep.* **7**, 13673 (2017).
68. Ma, J., Chen, X. & Sun, Q. microRNA-579 upregulation mediates death of human macrophages with mycobacterium tuberculosis infection. *Biochem. Biophys. Res. Commun.* **518**, 219–226 (2019).
69. Zhang, C. *et al.* Circular RNA circPPM1F modulates M1 macrophage activation and pancreatic islet inflammation in type 1 diabetes mellitus. *Theranostics* **10**, 10908–10924 (2020).
70. Zhou, R. *et al.* Comparative Analysis of Differentially Expressed Circular RNAs in Polarized Macrophages. *Front. Genet.* **13**, (2022).
71. Chen, Y. G. *et al.* Sensing Self and Foreign Circular RNAs by Intron Identity. *Mol.*

- Cell* **67**, 228-238.e5 (2017).
72. Liu, C.-X. *et al.* Structure and Degradation of Circular RNAs Regulate PKR Activation in Innate Immunity. *Cell* **177**, 865-880.e21 (2019).
73. Xia, P. *et al.* A Circular RNA Protects Dormant Hematopoietic Stem Cells from DNA Sensor cGAS-Mediated Exhaustion. *Immunity* **48**, 688-701.e7 (2018).
74. Xu, L. *et al.* HMGA2 regulates circular RNA ASPH to promote tumor growth in lung adenocarcinoma. *Cell Death Dis.* **11**, 593 (2020).
75. Wu, G. *et al.* CircASPH promotes KGN cells proliferation through miR-375/MAP2K6 axis in Polycystic Ovary Syndrome. *J. Cell. Mol. Med.* **26**, 1817–1825 (2022).
76. Meng, H. *et al.* Inhibition of circular RNA ASPH reduces the proliferation and promotes the apoptosis of hepatic stellate cells in hepatic fibrosis. *Biochem. Pharmacol.* **210**, 115451 (2023).
77. Xu, Y. *et al.* Circ_ASPH promotes cholangiocarcinoma growth and metastasis through the miR-581/ATP-binding cassette transporter G1 signaling pathway. *Cancer Commun.* **40**, 545–550 (2020).
78. Qu, Y., Qi, L., Hao, L. & Zhu, J. Upregulation of circ-ASPH contributes to glioma cell proliferation and aggressiveness by targeting the miR-599/AR/SOCS2-AS1 signaling pathway. *Oncol. Lett.* **21**, 388 (2021).
79. FERIOTTO, G. *et al.* Multiple Levels of Control of the Expression of the Human A β H-J-J Locus Encoding Aspartyl- β -hydroxylase, Junctin, and Junctate. *Ann. N. Y. Acad. Sci.* **1091**, 184–190 (2006).
80. Hong, C.-S., Kwon, S.-J. & Kim, D. H. Multiple functions of junctin and junctate, two distinct isoforms of aspartyl beta-hydroxylase. *Biochem. Biophys. Res. Commun.* **362**, 1–4 (2007).

81. Nagaoka, K. *et al.* Targeting Aspartate Beta-Hydroxylase with the Small Molecule Inhibitor MO-I-1182 Suppresses Cholangiocarcinoma Metastasis. *Dig. Dis. Sci.* **66**, 1080–1089 (2021).
82. Zou, Q. *et al.* Hydroxylase Activity of ASPH Promotes Hepatocellular Carcinoma Metastasis Through Epithelial-to-Mesenchymal Transition Pathway. *EBioMedicine* **31**, 287–298 (2018).
83. Rossi, D. *et al.* Multiple regions within junctin drive its interaction with calsequestrin-1 and its localization to triads in skeletal muscle. *J. Cell Sci.* **135**, (2022).
84. Guido, D., Demaurex, N. & Nunes, P. Junctate boosts phagocytosis by recruiting endoplasmic reticulum Ca²⁺ stores near phagosomes. *J. Cell Sci.* (2015) doi:10.1242/jcs.172510.
85. Schneider, C. A., Rasband, W. S. & Eliceiri, K. W. NIH Image to ImageJ: 25 years of image analysis. *Nat. Methods* **9**, 671–675 (2012).
86. Wu, H.-P., Shih, C.-C., Lin, C.-Y., Hua, C.-C. & Chuang, D.-Y. Serial increase of IL-12 response and human leukocyte antigen-DR expression in severe sepsis survivors. *Crit. Care* **15**, R224 (2011).
87. Trinchieri, G. Interleukin-12: A Proinflammatory Cytokine with Immunoregulatory Functions that Bridge Innate Resistance and Antigen-Specific Adaptive Immunity. *Annu. Rev. Immunol.* **13**, 251–276 (1995).
88. Weighardt, H. *et al.* Impaired Monocyte IL-12 Production Before Surgery as a Predictive Factor for the Lethal Outcome of Postoperative Sepsis. *Ann. Surg.* **235**, 560–567 (2002).
89. Liang, W. *et al.* Interleukin-5 deletion promotes sepsis-induced macrophage differentiation, deteriorates cardiac dysfunction, and exacerbates cardiac injury via the NF- κ B p65 pathway in mice. *BioFactors* **46**, 1006–1017 (2020).

90. Linch, S. N. *et al.* Interleukin 5 Is Protective during Sepsis in an Eosinophil-Independent Manner. *Am. J. Respir. Crit. Care Med.* **186**, 246–254 (2012).
91. Genin, M., Clement, F., Fattaccioli, A., Raes, M. & Michiels, C. M1 and M2 macrophages derived from THP-1 cells differentially modulate the response of cancer cells to etoposide. *BMC Cancer* **15**, 577 (2015).
92. Hu, X., Chakravarty, S. D. & Ivashkiv, L. B. Regulation of interferon and Toll-like receptor signaling during macrophage activation by opposing feedforward and feedback inhibition mechanisms. *Immunol. Rev.* **226**, 41–56 (2008).
93. Sancéau, J., Kaisho, T., Hirano, T. & Wietzerbin, J. Triggering of the Human Interleukin-6 Gene by Interferon- γ and Tumor Necrosis Factor- α in Monocytic Cells Involves Cooperation between Interferon Regulatory Factor-1, NF κ B, and Sp1 Transcription Factors. *J. Biol. Chem.* **270**, 27920–27931 (1995).
94. Yang, Y.-F., Tomura, M., Ono, S., Hamaoka, T. & Fujiwara, H. Requirement for IFN- γ in IL-12 production induced by collaboration between V α 14⁺ NKT cells and antigen-presenting cells. *Int. Immunol.* **12**, 1669–1675 (2000).
95. Valente, A. J. *et al.* A Complex Element Regulates IFN- γ -Stimulated Monocyte Chemoattractant Protein-1 Gene Transcription. *J. Immunol.* **161**, 3719–3728 (1998).
96. Bozza, F. A. *et al.* Cytokine profiles as markers of disease severity in sepsis: a multiplex analysis. *Crit. Care* **11**, R49 (2007).
97. MERA, S. *et al.* Multiplex cytokine profiling in patients with sepsis. *APMIS* **119**, 155–163 (2011).
98. Ashwal-Fluss, R. *et al.* circRNA Biogenesis Competes with Pre-mRNA Splicing. *Mol. Cell* **56**, 55–66 (2014).
99. Abdelmohsen, K. *et al.* Identification of HuR target circular RNAs uncovers suppression of PABPN1 translation by CircPABPN1. *RNA Biol.* **14**, 361–369

(2017).

100. Wang, X. & Bai, M. CircTM7SF3 contributes to oxidized low-density lipoprotein-induced apoptosis, inflammation and oxidative stress through targeting miR-206/ASPH axis in atherosclerosis cell model in vitro. *BMC Cardiovasc. Disord.* **21**, 51 (2021).
101. Chow, S. H., Deo, P. & Naderer, T. Macrophage cell death in microbial infections. *Cell. Microbiol.* **18**, 466–474 (2016).
102. Du, W. W. *et al.* Induction of tumor apoptosis through a circular RNA enhancing Foxo3 activity. *Cell Death Differ.* **24**, 357–370 (2017).
103. Tedesco, S. *et al.* Convenience versus Biological Significance: Are PMA-Differentiated THP-1 Cells a Reliable Substitute for Blood-Derived Macrophages When Studying in Vitro Polarization? *Front. Pharmacol.* **9**, (2018).

Supplementary Material

Table S1 Patient demographic and clinical information.

ID	Sex	Age	ICU LOS (days)	MODS score	Pathogen	Co-morbidities
1	F	39	11	3	group A strep	fibromyalgia, infectious colitis, chronic anemia, GERD
2	M	68	4	Unknown	<i>A. turicensis</i> + coag. neg. <i>Staphylococcus</i>	diverticulosis, hypertension, hyperlipidemia, fatty liver
3	F	70	9	Unknown	MRSA	ESRD, hypertension, T2DM, celiac, CHF, COPD
4	F	73	14	3	<i>S. anginosus</i> group, <i>S. epidermidis</i> , <i>Pseudomonas</i> , coag. neg. <i>Staph</i>	hypertension, Calcium pyrophosphate dihydrate (CPPD) arthropathy
5	M	55	3	1	<i>S. aureus</i>	IV drug use, alcohol abuse, leg abscess
6	F	71	1	2	Unknown	Unknown
7	F	74	3	2	<i>S. pneumoniae</i>	Unknown

* Information for one patient was unable to be retrieved at the time of writing.

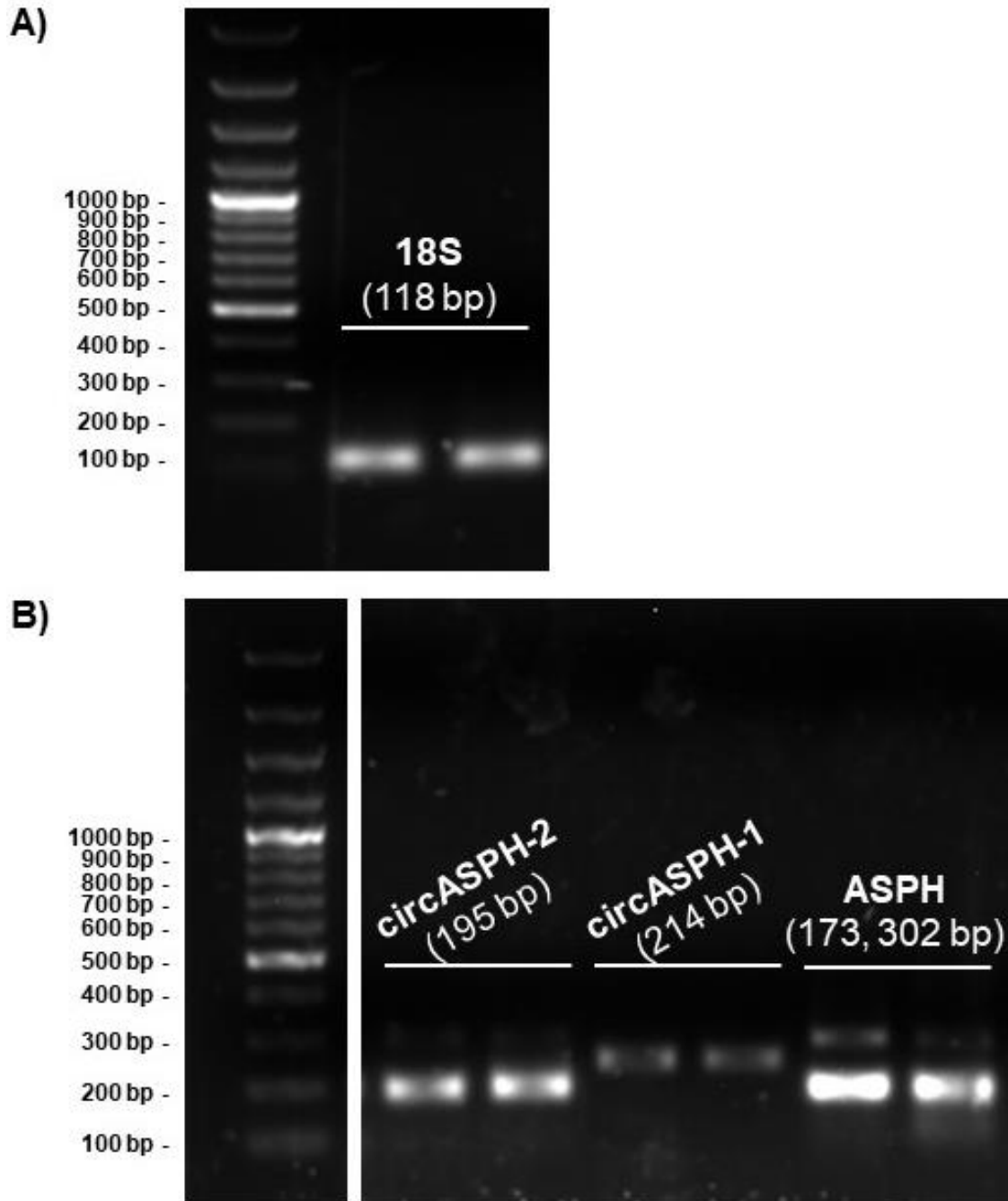


Figure S1 Validation of PCR products for 18S, circASPH and ASPH. THP-1 cells were differentiated with 25 ng/mL PMA for 48 h and rested in PMA-free media for 24 h. Total RNA was harvested and cDNA was synthesized. Quantitative PCR products for 18S (**A**), two isoforms of circASPH, and ASPH (**B**) were run on a 1.5 % agarose gel containing SYBR™ Safe DNA gel stain, and resulting bands were visualized. Bands are labelled with their target and expected sizes, alongside a 100 bp DNA ladder.

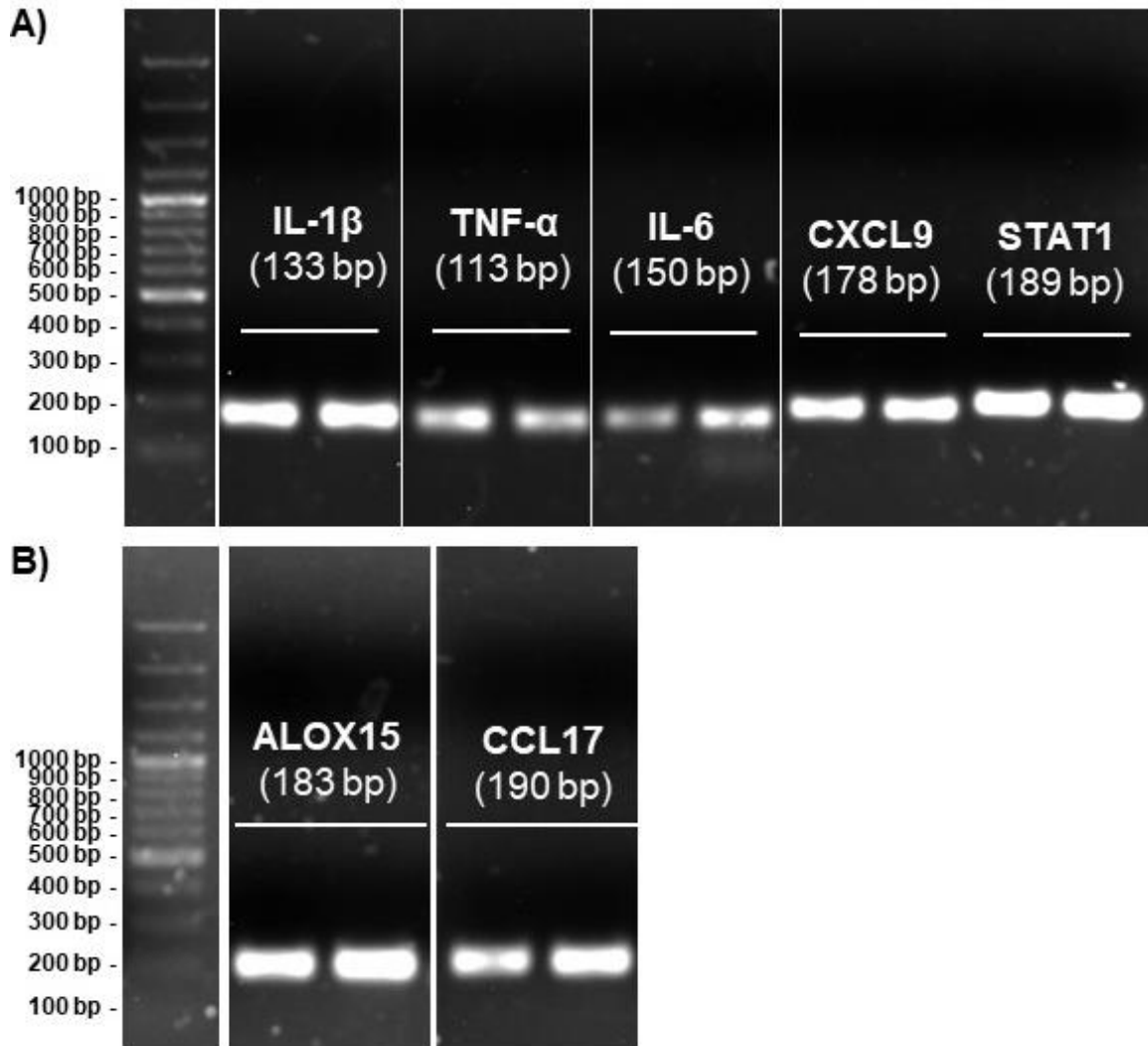


Figure S2 Validation of PCR products for M1 and M2 gene markers. THP-1 cells were differentiated with 25 ng/mL PMA for 48 h and rested in PMA-free media for 24 h, then treated with 20 ng/mL IFN- γ + 5 ng/mL LPS or 30 ng/mL IL-4 for 1 d. Total RNA was harvested and cDNA was synthesized. Quantitative PCR products for M1 gene markers after IFN- γ + LPS stimulation (**A**) or M2 gene markers after IL-4 stimulation (**B**) were run on a 1.5 % agarose gel containing SYBRTM Safe DNA gel stain, and resulting bands were visualized. Bands are labelled with their target and expected sizes, alongside a 100 bp DNA ladder.

siRNA **UCAAAUAAUCUCUGUUU-5'**
 |||||
TGATGCCAAAGTTTTATTAGAGACAAAGCATGGAGGACAC
circASPH BSJ

UCAAAUAAUCUCUGUUU-5'
 | |||||
CAAAATGGCTGAAGATAAAGAGACAAAGCATGGAGGACAC
 Linear ASPH exons 2/3

UCAAAUAAUCUCUGUUU-5'
 ||||| ||
TGATGCCAAAGTTTTATTAGGACTTAAAGAGAGATCTACT
 Linear ASPH exons 5/6

Figure S3 CircASPH siRNA binding to circASPH and linear ASPH.

Curriculum Vitae

Name:	Tan Ze Wang
Post-secondary Education and Degrees:	The University of Western Ontario London, Ontario, Canada 2017-2021 B.MSc.
	The University of Western Ontario London, Ontario, Canada 2021-2023 M.Sc. Pathology and Laboratory Medicine
Honours and Awards:	Canada Graduate Scholarship – Master’s (NSERC) 2022-2023
	Dr. Fredrick Winnet Luney Graduate Research Award 2022
Related Work Experience	Pre-Graduate Student - Research University Hospital, London, Ontario 2021
	Teaching Assistant The University of Western Ontario 2022

Conference Abstracts:

Wang T, Yu F, Warsi A, Rong K, Mele T, Zheng X. Alterations in circular RNA landscape in septic peripheral blood mononuclear cells before and after intensive care. Expected poster presentation at the 23rd Annual Meeting of the Federation of Clinical Immunology Societies (FOCIS 2023). June 2023.

Wang T, Zheng X. Role of circular RNA ASPH in macrophage function and response in sepsis. Poster presentation at Schulich School of Medicine and Dentistry Department of Pathology Research Day, March 2023.

Wang T, Yu F, Warsi A, Rong K, Mele T, Zheng X. Characterization of differentially expressed circular RNAs in septic PBMCs. Poster presentation at Schulich School of Medicine and Dentistry Department of Surgery Research Day, June 2022.

Wang T, Yu F, Warsi A, Rong K, Mele T, Zheng X. Characterization of differentially expressed circular RNAs in septic PBMCs. Poster presentation at London Health Research Day, May 2022. Virtual meeting.